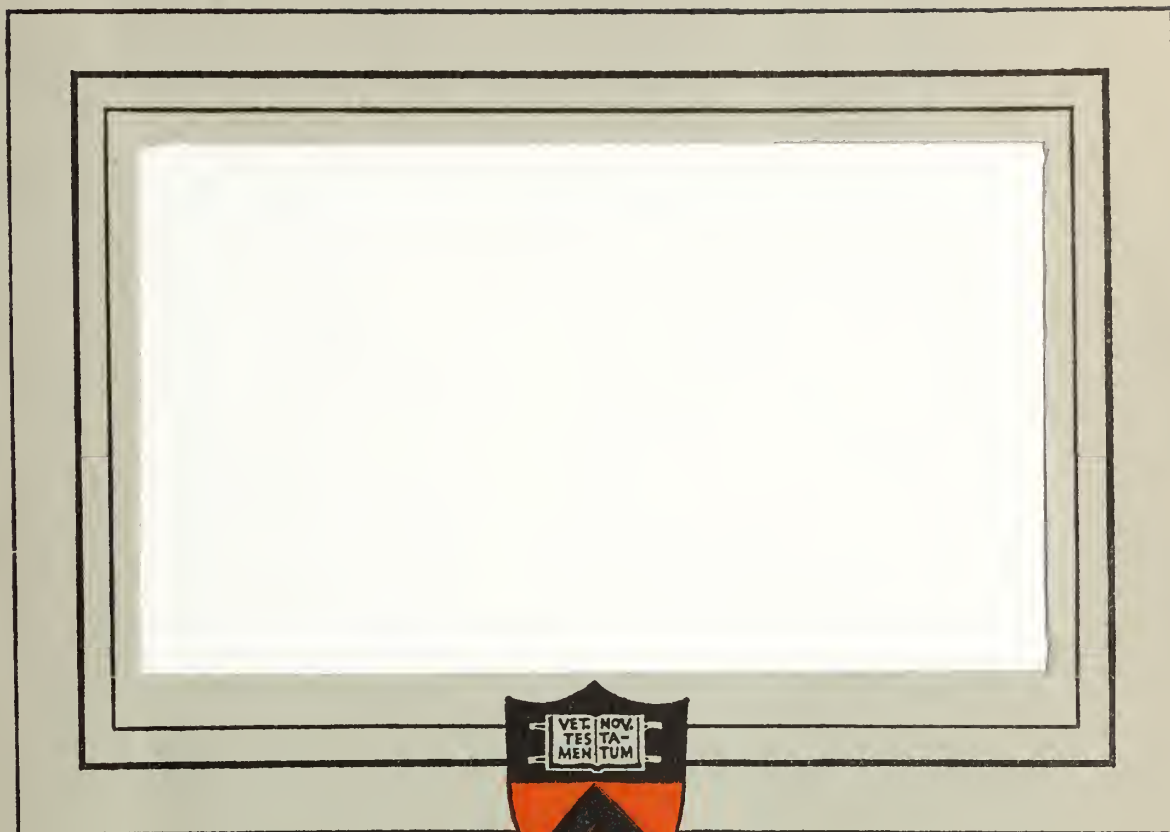


NPS ARCHIVE  
1965  
FINNERAN, W.



Thesis  
F446

PRINCETON UNIVERSITY

DEPARTMENT OF  
AEROSPACE AND MECHANICAL SCIENCES

Monterey  
U. S. Naval Postgraduate School  
Monterey, California

**DUDLEY KNOX LIBRARY**  
**NAVAL POSTGRADUATE SCHOOL**  
**MONTEREY CA 93943-5101**



A SIMULATOR STUDY OF A NONLINEAR ROLL  
DAMPER FOR THE F-8 AIRPLANE IN THE  
CARRIER APPROACH MANEUVER

by

W. J. Finneran, Lieutenant Commander, USN

and

R. A. Fidler, Lieutenant, USN

Princeton University  
School of Engineering and Applied Sciences  
Aerospace and Mechanical Sciences Department

Report No. 728

May 1965

Submitted in partial fulfillment of the requirements for the degree  
of Master of Science in the Department of Aerospace and Mechanical  
Sciences, Princeton University.

Signatures of authors:



## ACKNOWLEDGEMENT

The authors wish to express their gratitude to Mr. Theodor A. Dukes, Research Aeronautical Engineer, Instrumentation and Control Laboratory, Princeton University.

Mr. Dukes suggested this investigation and designed the electronic circuitry which is essential to the carrier approach simulator display.

For his advice and guidance we offer our sincere appreciation.



## TABLE OF CONTENTS

	Page
ACKNOWLEDGEMENT	i
LIST OF TABLES	iii
LIST OF FIGURES	iv
NOMENCLATURE	v
SUMMARY	x
I. INTRODUCTION	1
II. FLIGHT SIMULATOR	3
A. EQUIPMENT	3
B. AIRPLANE EQUATIONS OF MOTION	4
YAW STABILITY AUGMENTATION SYSTEM	8
ROLL DAMPER SYSTEM	11
C. FLIGHT PATH GEOMETRY	12
D. CARRIER APPROACH SIMULATOR DISPLAY	15
E. SIMULATED ATMOSPHERIC TURBULENCE	21
III. FLIGHT EXPERIMENTS	24
A. PROCEDURES	24
B. EVALUATION OF THE FLIGHT SIMULATOR	26
C. NONLINEAR ROLL DAMPER INVESTIGATION	32
IV. CONCLUSIONS AND RECOMMENDATIONS	37
REFERENCES	39
TABLES	
FIGURES	



LIST OF TABLES

- I. COOPER PILOT OPINION RATING SYSTEM
- II. PILOT FLIGHT EXPERIENCE SUMMARY
- III. F-8 AIRPLANE DATA
- IV. AIRPLANE STABILITY DERIVATIVES FROM REFERENCE 7.
- V. DISPLAY RANGE FUNCTIONS
- VI. SIMULATED ATMOSPHERIC TURBULENCE
- VII. RESULTS OF FLIGHT IN EVALUATION OF THE SIMULATOR
- VIII. RESULTS OF ROLL DAMPER CONFIGURATION EVALUATION AT MODERATE TURBULENCE LEVEL
- IX. RESULTS OF ROLL DAMPER CONFIGURATION EVALUATION AT SEVERE TURBULENCE LEVEL



## LIST OF FIGURES

1. CARRIER APPROACH SIMULATOR SET-UP
2. CARRIER APPROACH SIMULATOR FUNCTIONAL DIAGRAM
3. LONGITUDINAL ANALOG COMPUTER DIAGRAM
4. LATERAL-DIRECTIONAL ANALOG COMPUTER DIAGRAM
5. F-8 AIRPLANE X-AXIS
6. YAW STABILITY AUGMENTATION TRANSFER FUNCTION
7. YAW STABILITY SYSTEM COMPUTER DIAGRAM
8. VARIATION OF ROLL DAMPER GAINS WITH LATERAL STICK POSITION
9. ROLL DAMPER SYSTEM COMPUTER DIAGRAM
10. VECTOR DIAGRAM OF APPROACH
11. DETAILS OF THE RELATIVE FLIGHT PATH
12. FRESNEL LENS OPTICAL LANDING SYSTEM GEOMETRY
13. PILOT'S VISUALIZATION OF LATERAL DISPLACEMENT
14. PILOT'S VISUALIZATION OF YAW
15. CARRIER APPROACH SIMULATOR DISPLAY
16. VIEWING ANGLE THROUGH FRONT WINDSCREEN DURING CARRIER APPROACH
17. DONNER COMPUTER SET-UP
18. DISPLACEMENT VS. COOPER RATING FROM EVALUATION OF SIMULATOR DATA
19. TYPICAL TIME HISTORY OF SIMULATED APPROACH (MODERATE TURBULENCE)
20. TYPICAL TIME HISTORY OF SIMULATED APPROACH (SEVERE TURBULENCE)



## NOMENCLATURE

$C_L$  Lift coefficient, lift/ $qS$

$C_m$  Pitching moment coefficient, pitching moment/ $qS\bar{c}$

$C_{l\ell}$  Rolling moment coefficient, rolling moment/ $qS\bar{c}$

$C_n$  Yawing moment coefficient, yawing moment/ $qS\bar{c}$

$C_y$  Lateral force coefficient, lateral force/ $qS$

$$C_{L\alpha} = \frac{\partial C_L}{\partial \alpha} \qquad C_{l_p} = \frac{\partial C_{l\ell}}{\partial \left(\frac{pb}{2V_0}\right)}$$

$$C_{L\delta_e} = \frac{\partial C_L}{\partial \delta_e} \qquad C_{l_r} = \frac{\partial C_{l\ell}}{\partial \left(\frac{rb}{2V_0}\right)}$$

$$C_{m\alpha} = \frac{\partial C_m}{\partial \alpha} \qquad C_{l_\beta} = \frac{\partial C_{l\ell}}{\partial \beta}$$

$$C_{m\dot{\alpha}} = \frac{\partial C_m}{\partial \left(\frac{\dot{\alpha}\bar{c}}{2V_0}\right)} \qquad C_{l\delta_a} = \frac{\partial C_{l\ell}}{\partial \delta_a}$$

$$C_{m\delta_e} = \frac{\partial C_m}{\partial \delta_e} \qquad C_{l\delta_r} = \frac{\partial C_{l\ell}}{\partial \delta_r}$$

$$C_{m_q} = \frac{\partial C_m}{\partial \left(\frac{q\bar{c}}{2V_0}\right)} \qquad C_{n_r} = \frac{\partial C_n}{\partial \left(\frac{rb}{2V_0}\right)}$$

$$C_{y_\beta} = \frac{\partial C_y}{\partial \beta} \qquad C_{n_p} = \frac{\partial C_n}{\partial \left(\frac{pb}{2V_0}\right)}$$

$$C_{y_p} = \frac{\partial C_y}{\partial \left(\frac{pb}{2V_0}\right)} \qquad C_{n\delta_a} = \frac{\partial C_n}{\partial \delta_a}$$

$$C_{y\delta_r} = \frac{\partial C_y}{\partial \delta_r} \qquad C_{n\delta_r} = \frac{\partial C_n}{\partial \delta_r}$$



$$\frac{L_\alpha}{V_o} = \frac{g}{V_o C_{L_o}} C_{L_\alpha}$$

$$\frac{L_{\delta e}}{V_o} = \frac{g}{V_o C_{L_o}} C_{L_{\delta e}}$$

$$M_\alpha = \frac{g}{\bar{c} C_{L_o} \left(\frac{k_y}{\bar{c}}\right)^2} C_{m_\alpha}$$

$$M_\alpha = \frac{g}{2V_o C_{L_o} \left(\frac{k_y}{\bar{c}}\right)^2} C_{m_\alpha}$$

$$M_\theta = \frac{g}{2V_o C_{L_o} \left(\frac{k_y}{\bar{c}}\right)^2} C_{m_q}$$

$$M_{\delta e} = \frac{g}{C_{L_o} \bar{c} \left(\frac{k_y}{\bar{c}}\right)^2} C_{m_{\delta e}}$$

$$k_y = \left[ \frac{I_y g}{W} \right]^{1/2}$$

$$Y_v = \frac{g}{V_o C_{L_o}} C_{y_\beta}$$

$$Y_p = \frac{g}{C_{L_o}} C_{y_p}$$

$$Y_r = \frac{g}{C_{L_o}} C_{y_r}$$

$$Y_{\delta r} = \frac{g}{C_{L_o}} C_{y_{\delta r}}$$

$$L_p = \frac{g}{2V_o C_{L_o}} \frac{C_{l_p}}{\left(\frac{k_x}{b}\right)^2}$$

$$L_r = \frac{g}{2V_o C_{L_o}} \frac{C_{l_r}}{\left(\frac{k_x}{b}\right)^2}$$

$$L_v = \frac{g}{bV_o C_{L_o}} \frac{C_{l_\beta}}{\left(\frac{k_x}{b}\right)^2}$$

$$L_{\delta a} = \frac{g}{bC_{L_o}} \frac{C_{l_{\delta a}}}{\left(\frac{k_x}{b}\right)^2}$$

$$L_{\delta r} = \frac{g}{bC_L} \frac{C_{l_{\delta r}}}{\left(\frac{k_x}{b}\right)^2}$$

$$N_r = \frac{g}{2V_o C_{L_o}} \frac{C_{n_r}}{\left(\frac{k_z}{b}\right)^2}$$

$$N_p = \frac{g}{2V_o C_{L_o}} \frac{C_{n_p}}{\left(\frac{k_z}{b}\right)^2}$$

$$N_v = \frac{g}{bV_o C_{L_o}} \frac{C_{n_\beta}}{\left(\frac{k_z}{b}\right)^2}$$

$$N_{\delta a} = \frac{g}{bC_{L_o}} \frac{C_{n_{\delta a}}}{\left(\frac{k_z}{b}\right)^2}$$

$$N_{\delta r} = \frac{g}{bC_{L_o}} \frac{C_{n_{\delta r}}}{\left(\frac{k_z}{b}\right)^2}$$



$a_y$	lateral acceleration, feet/second <sup>2</sup>
AW	ambient wind, kts
$a_z$	normal acceleration, feet/second <sup>2</sup>
b	wing span, feet
c.g.	airplane center of gravity
$\bar{c}$	mean aerodynamic chord, feet
d	lateral displacement, feet
g	gravitational constant, feet/second <sup>2</sup>
h	vertical displacement, feet
$I_{XX}$	moment of inertia about the principal x axis, slug-feet <sup>2</sup>
$I_x$	moment of inertia about the stability x axis, slug-feet <sup>2</sup>
$I_{YY}$	moment of inertia about the principal y axis, slug-feet <sup>2</sup>
$I_y$	moment of inertia about the stability y axis, slug-feet <sup>2</sup>
$I_{ZZ}$	moment of inertia about the principal z axis, slug-feet <sup>2</sup>
$I_z$	moment of inertia about the stability z axis, slug-feet <sup>2</sup>
m	airplane mass, slugs
$n_y$	lateral acceleration, $a_y/g$
$n_z$	normal acceleration, $-a_z/g$
$p=\dot{\phi}$	rolling velocity, radians/second
$\dot{p}=\ddot{\phi}$	rolling acceleration, radians/second <sup>2</sup>
$q=\dot{\theta}$	pitching velocity, feet/second <sup>2</sup>
$\dot{q}=\ddot{\theta}$	pitching acceleration, radians/second <sup>2</sup>
R	range, feet
$r=\dot{\psi}$	yawing velocity, feet/second <sup>2</sup>
$\dot{r}=\ddot{\psi}$	yawing acceleration, radians/second <sup>2</sup>



S	wing area, square feet
(SF)	display scale factor
t	time, seconds
$U_S$	aircraft carrier speed, kts
$u_i$	oscilloscope display dimensions, cm
$V_O$	initial airplane airspeed, feet/second
v	lateral velocity, feet/second
W	airplane weight, pounds
w	vertical velocity, feet/second
WOD	wind over deck, kts
$\alpha$	angle of attack, radians
$\beta$	sideslip angle, radians
$\dot{\beta}$	rate of change of sideslip angle, radians/second
$\gamma$	actual glide slope angle, degrees
$\delta$	control surface deflection, radians
$\eta_i$	flight path and simulator display geometric angles
$\theta$	pitch angle, radians
$\lambda$	wavelength, feet
$\rho$	air density, slugs/foot <sup>3</sup>
$\varphi$	bank angle, radians
$\psi$	yaw angle, radians

### Subscripts

a	aileron
e	elevator
r	rudder



Subscripts

- g gust (atmospheric turbulence)
- o (zero) initial condition or initial value

Prescript

- $\Delta$  ( $\delta$ ) perturbation in motion indicated by symbol following



## SUMMARY

This study is concerned with the development and evaluation of a six degree of freedom flight simulator and its use in an investigation of a nonlinear control system. Linearized equations of motion to describe the LING TEMPCO VOUGHT F-8 airplane in the carrier approach maneuver formed the basis of the flight simulator development. The equations of motion were mechanized on an analog computer. The airplane motion variables from the analog computer were combined with appropriate nonlinear functions of range to form the display of the flight simulator. The display presents the horizon, the meatball of the FLOLS, and the deck centerline and ramp of the aircraft carrier.

Experienced Navy pilots flew all the simulated carrier approaches conducted during this investigation. The pilots' opinion ratings and performance were the basis of the analysis. Pilot opinion ratings were based on the Cooper rating system, and pilot-airplane performance was measured as the vertical and lateral deviation from the desired glide path, at the termination of the approach.

The evaluation of the simulator indicated that, by comparison with actual flight information, the simulator is capable of reproducing actual flight information with meaningful correspondence, when there are non-trivial differences in the parameters being investigated. It was also indicated that there is some direct correspondence between average pilot-airplane lateral-directional performance and pilot opinion rating.

The second phase of the study was concerned with the use of the flight simulator to investigate some parameters of a nonlinear roll



damper system of the type employed in the F-8 airplane. The simulated F-8 airplane flights in "moderate" atmospheric turbulence indicated no clear preference in the roll damper configurations tested. Only in the simulator flights in "severe" atmospheric turbulence did any clear preference as to the configuration of the roll damper emerge. Among the configurations tested, the system currently installed in the F-8 airplane was preferred. Since all the systems tested provided more damping and less maneuverability than the current F-8 airplane system, a study should be undertaken to determine if a system which provides less damping and more maneuverability may prove to be a superior system.



## I. INTRODUCTION

The aircraft carrier approach is one of the most exacting pilot tasks in aviation today. This task is made more difficult by the relatively poor low speed stability and handling qualities of current high performance jet aircraft. This situation has created the need for stability augmentation systems, especially for use in the power approach configuration of the airplane. The choice of a stability augmentation system requires a compromise between desired stability and required maneuverability, especially when there is some limitation on control power. One possible solution is the application of nonlinear damping. The damping feedback gain can be made a function of the pilots' control stick position. The feedback gain is high when the pilots' stick deflections are small, and when the pilot uses large stick deflection for maneuvering, the feedback gain is diminished or entirely removed. This principle of nonlinear damping is the theme of this study. Since the LING TEMPCO VOUGHT F-8 airplane currently employs a roll damper system based on the nonlinear division of roll rate authority between pilot and roll damper system, it was decided to make the F-8 airplane and roll damper system the basis for the investigation.

As the first phase of such an investigation a six degree of freedom, fixed base flight simulator was developed and evaluated. This flight simulator places a human "pilot" in the situation of controlling a high performance jet airplane in a standard aircraft carrier approach maneuver under variable atmospheric turbulence. The approach task is characterized by the requirement to fly the simulator with minimum deviations in altitude



and lateral displacement from the desired glide slope and carrier deck centerline respectively, in order to make a satisfactory landing. The magnitude of these deviations at the termination of the approach can be considered a measure of pilot-airplane performance.

The second phase of the investigation was concerned with the study of some parameters of a nonlinear roll damper system of the type employed in the F-8 airplane. The system operates as a control stick governed gain in the negative feedback of roll rate to aileron deflection. This initial investigation was limited to the evaluation of some basic parameters of the nonlinear gain function. These parameters are discussed in detail in section III C. Pilot opinions of the handling qualities of the simulated airplanes were based on the Cooper rating system, which is reported on in Ref. 1. Table I is a brief outline of the Cooper rating system which was utilized. Table II briefly summarizes the flight experience of the pilots who were engaged for this study.



## II. FLIGHT SIMULATOR

### A. EQUIPMENT

The carrier approach simulator, and the investigation pertaining thereto, required the use of various electrical and electronic equipment, of which the PACE TR-48 analog computer was the primary element. Fig. 1 shows a photograph of the simulator system which includes these various items to be described in detail below.

Fig. 2 shows a functional block diagram arrangement of the equipment used in this study. The PACE TR-48 analog computer (Electronics Associates, Inc.) is a solid state computer with fifty-eight operational amplifiers and sixty potentiometers. Some of this capacity was utilized for the airplane equations of motion and the remaining capacity was used for generating the simulator display signals.

Also used was the DONNER MODEL 3100 analog computer. This computer contains thirty operational amplifiers and forty potentiometers, and was used in conjunction with three MODEL 3751 function generators. These function generators supplied nonlinear functions of range which controlled deck growth, lateral displacement, and the meatball sensitivity of the display during the approach maneuver.

The cockpit simulator consists of a seat, control stick, rudder pedals and throttle with quadrant, all mounted in a wooden chassis or framework. This piece of equipment is full scale, in that it allows the pilot to sit in the seat and "control" the progress of the simulated approach. Attached to all cockpit simulator controls are 100K $\Omega$  potentiometers. These potentiometers are center-tapped and supplied with reference voltages of  $\pm 10$  volts.



The potentiometers are used for signal generation proportional to rudder pedal and control stick deflections to be introduced into the airplane equations of motion which are set up on the TR-48 computer.

The display is a simulation of the pilot's view from the cockpit during a carrier approach and is seen on an eight centimeter by ten centimeter screen of a TEKTRONICS, INC. cathode ray oscilloscope.

The complete simulator set-up has the capability of having noise introduced to simulate air turbulence during the approach task. Airplane response to turbulence and pilot control is seen as appropriate displacements of carrier deck and horizon on the display. The noise (turbulence) was obtained from a two channel magnetic tape recording of Gaussian noise which emanated from a low frequency noise generator. The Magnecord tape recorder transport was used in conjunction with a modulator and demodulator for recording the original tape and playing back the tape during simulated approaches.

A six channel Brush recorder was used to graph responses of airplane to turbulence and control inputs and to evaluate the quality of the simulated approaches.

Fig. 2 shows the relationship and utilization of the equipment described above in simple block diagram form, with brief descriptions of individual signals on interconnecting lines.

#### B. AIRPLANE EQUATIONS OF MOTION

The equations used to describe the airplane's motion during the final approach to a carrier landing are the usual linear, constant coefficient, differential equations derived from Newton's law by means of the small perturbation theory. The use of these equations to describe the airplane



motions assumes that atmospheric turbulence and control surface deflections cause only small perturbations to the airplane's steady state flight condition. The equations of motion are written for longitudinal motion and lateral-directional motion, with the assumption that there is no cross coupling between the two sets of equations. The validity of these assumptions lies in the fact that the final portion of a carrier approach, after intercepting and trimming the airplane onto the glide slope, is an unaccelerated, constant airspeed, shallow descent to the landing. In order to make a satisfactory landing approach the airplane's deviations from the prescribed flight path must be small, thus they are approximately small perturbations from the desired steady state flight path.

The equations of motion are developed in real time notation since a pilot was required to "fly" the simulator.

The lateral-directional handling qualities of the airplane were the primary concern of this study, so that a simplified set of longitudinal equations was used. The longitudinal degrees of freedom were added to the simulator primarily to increase the piloting task. In the development of the longitudinal equations of motion it was assumed that airspeed was held constant and therefore, only the lift and pitching moment equations were required to describe the airplane's longitudinal motion. The use of only the lift and pitching moment equations yields a reasonable approximation to the airplane's short period motion while eliminating the phugoid mode entirely. This approximation, since the drag equation has been dropped, may be thought of as though the drag equation is satisfied instantaneously by an automatic throttle configuration which maintains constant airspeed.



The elimination of the phugoid mode of motion is reasonable since the airplane response to the phugoid excitation is suppressed under the exacting pilot control required in a carrier approach.

The equations of motion are written in a stability axis system where the X-axis is aligned initially with the steady state relative wind. This choice of axis systems eliminates the vertical velocity component caused by the airplane's descent to the landing by placing the X-axis along the desired glide slope. This approximation to the condition that the steady state flight path be nearly horizontal is assumed valid in that the glide slope angle is approximately three degrees.

The resultant dimensional equations describing the airplane motion are written in the notation of Ref. 2. After division by the coefficient of the highest derivative the equations of motion take the following form:

#### Longitudinal

(a) Lift equation:

$$\Delta \dot{\alpha} - \Delta \dot{\theta} + \frac{L_{\alpha}}{V_0} \Delta \alpha + \frac{L_{\delta_e}}{V_0} \Delta \delta_e = 0 \quad (1)$$

(b) Pitching moment equation:

$$\Delta \dot{\theta} - M_{\dot{\theta}} \Delta \dot{\theta} - M_{\dot{\alpha}} \Delta \dot{\alpha} - M_{\alpha} \Delta \alpha - M_{\delta_e} \Delta \delta_e = 0 \quad (2)$$

#### Lateral-Directional

(a) Side force equation:

$$\Delta \dot{\beta} - Y_v \Delta \beta - \frac{Y_p}{V_0} \Delta \dot{\phi} - \frac{g}{V_0} \Delta \phi + \frac{(V_0 - Y_r)}{V_0} \Delta \dot{\psi} - \frac{Y_{\delta_r}}{V_0} \Delta \delta_r = 0 \quad (3)$$

(b) Rolling moment equation:

$$\Delta \dot{\phi} - L_p \Delta \dot{\phi} - \frac{I_{xz}}{I_x} \Delta \dot{\psi} - L_r \Delta \dot{\psi} - L_v V_0 \Delta \beta - L_{\delta_a} \Delta \delta_a - L_{\delta_r} \Delta \delta_r = 0 \quad (4)$$



(c) Yawing moment equation:

$$\Delta \dot{\psi}' - N_r \Delta \dot{\psi} - \frac{I_{xz}}{I_z} \Delta \dot{\phi}' - N_p \Delta \dot{\phi} - N_v V_o \Delta \beta - N_{\delta_a} \Delta \delta_a - N_{\delta_r} \Delta \delta_r = 0 \quad (5)$$

For the remainder of the report the  $\Delta$  notation will be dropped for brevity, with the knowledge that all motion variables are assumed to be small perturbations from the steady state condition.

Vertical displacement of the airplane, with respect to the desired glide slope, is required as part of the simulator display. The airplane's displacement from the desired glide slope was determined by rearranging the lift equation (1) so as to yield normal acceleration:

$$a_z = -L_\alpha \alpha + L_{\delta_e} \delta_e \quad (1a)$$

The double integration of normal acceleration yields the desired displacement from the glide slope.

The two uncoupled sets of equations and the normal acceleration equation were programmed for the TR-48 analog computer; program diagrams are presented in Fig. 3 and Fig. 4.

The coefficients of the equations of motion, for the F-8 airplane in the power approach configuration, were determined from stability derivatives supplied to the Bureau of Naval Weapons by the Ling Temco Vought Corporation. Information utilized from this report is reproduced in Table III.

The use of the stability axis system requires the airplane's moments and products of inertia to be calculated based on the stability axes. This made it necessary to transform the moments of inertia from the principal axes to the stability axes; the stability X-axis being 6.4 degrees nose down from the principal X-axis (Fig. 5). The equations of motion and the normal



acceleration equation, with numerical values of the coefficients for the basic F-8 airplane become:

Longitudinal

(a) Lift equation:

$$\dot{\alpha} - \dot{\theta} + .398 \alpha + .0596 \delta_e = 0 \quad (6)$$

(b) Pitching moment equation:

$$\dot{\theta} + .351 \dot{\theta} + .043 \dot{\alpha} + 1.18 \alpha + 2.6 \delta_e = 0 \quad (7)$$

Normal Acceleration:

$$a_z = - 93.5 \alpha + 14.0 \delta_e \quad (6a)$$

Lateral-Directional

(a) Side force equation:

$$\dot{\beta} + .193 \beta - .063 \dot{\phi} - .137 \phi + .96 \dot{\psi} - .035 \delta_r = 0 \quad (8)$$

(b) Rolling moment equation:

$$\dot{\phi} + 1.62 \dot{\phi} + .91 \dot{\psi} - .875 \dot{\psi} + 14.35 \beta - 5.45 \delta_a - .768 \delta_r = 0 \quad (9)$$

(c) Yawing moment equation:

$$\dot{\psi} + .219 \dot{\psi} + .104 \dot{\phi} + .027 \dot{\phi} - 2.14 \beta + .218 \delta_a + 1.082 \delta_r = 0 \quad (10)$$

Some of the dimensional stability derivatives were changed to represent other airplane configurations during the evaluation of the simulator; these dimensional stability derivatives are listed in Table IV.

Yaw stability augmentation system

The yaw stabilization system presently in use on the F-8 airplane is described by the following transfer function:

$$\frac{\delta_r}{n_y} = \frac{s(s + 5.45)}{(s + 1.735)(s + 13.6)} \quad \text{radians/g} \quad (11)$$

Rearranging the transfer function into Bode form yields the following:



$$\frac{\delta_r}{n_y} = \frac{.231 s(\frac{s}{5.45} + 1)}{(\frac{s}{1.735} + 1)(\frac{s}{13.6} + 1)} \quad (12)$$

This transfer function is plotted as the solid lines in Fig. 6. In order to simplify the mechanization of the yaw stabilization system, and yet retain its effectiveness and predominant low frequency dynamic characteristics the following approximation was made:

$$\frac{\delta_r}{n_y} = \frac{.231s}{(\frac{s}{3.2} + 1)} = \frac{k s}{(T_s + 1)} \quad (13)$$

which is plotted as the dashed line in Fig. 6 and can be considered a reasonable approximation to the actual transfer function. It may be seen in Fig. 6 that the approximate transfer function is less than two db higher in amplitude than the exact function below frequencies of approximately 14 radians/second, and does not deviate more than three db from the exact function at all frequencies. At frequencies below three radians/second the phase angle of the approximation leads the exact function by less than six degrees, and does not deviate more than 16 degrees at frequencies above three radians/second. It should be noted that the natural frequencies of pilot and gust inputs, and airplane responses are generally at or below one cycle/second (6.28 radians/second); so that in this frequency range the approximate function deviates from the exact function by less than two db in amplitude and 12 degrees in phase.

In the F-8 airplane,  $n_y$  is measured by an accelerometer located at fuselage station 440 and waterline 91. The center of gravity of the airplane in the power approach configuration chosen for this analysis is at fuselage station 450 and water line 97; thus the accelerometer is ten inches forward and six inches below the c.g. of the airplane. It was



assumed that the accelerometer was located at the c.g. of the airplane. This approximation greatly simplified the mechanization of the yaw stabilization system and was considered to be in keeping with other assumptions made. It must be pointed out that the yaw stabilization system was required only to approximate the F-8 airplane and was not a direct part of the study of the nonlinear roll stabilization-aileron control system. With the approximation that the accelerometer was located at the airplane's c.g., the lateral acceleration measured by the accelerometer becomes:

$$n_y = \frac{V_0 Y_v}{g} \beta + \frac{Y \delta_r}{g} \delta_r \quad (14)$$

The lateral acceleration, with numerical values for the coefficients, becomes:

$$n_y = - 1.405\beta + .256\delta_r \quad (15)$$

Combining equations (13) and (14) the complete form of the yaw stabilization transfer function becomes:

$$\delta_r = \left[ \frac{kV_0 Y_v}{g} \beta + \frac{kY \delta_r}{g} \delta_r \right] \frac{s}{T_s + 1} \quad (16)$$

The yaw stabilization system computer diagram is presented in Fig. 7. This form of yaw stabilization was maintained throughout the study.

It may be noted, by examination of equation (16) and Fig. 7, that the yaw stabilization of the F-8 airplane is in reality a "turn coordinator." With no rudder input by the pilot, any lateral acceleration must be the result of sideslip. The lateral acceleration will cause a rudder deflection appropriate to cancel the sideslip and the resultant lateral



acceleration. It may also be noted that this type of yaw stabilization allows the pilot to command a steady sideslip of the airplane by deflecting the rudder. For straight line flight the resultant steady sideslip may be seen by setting  $n_y$  equal to zero in equation (14).

#### Roll damper system

The roll damper system in use on the F-8 airplane is a nonlinear function of lateral control stick position, and is described by the transfer function:

$$\delta_a = K_p(\delta_s)p \tag{17}$$

where  $K_p$  is the roll damper gain dependent on lateral control stick position ( $\delta_s$ ). With the lateral control stick centered the roll damper gain is high, and the roll damper system provides its maximum reduction of roll rate due to atmospheric turbulence. This high gain would be undesirable when the pilot needs to maneuver the airplane rapidly, since the airplane's response to the pilot's lateral stick deflections would be very sluggish. Therefore, the roll damper gain is decreased with lateral stick position when the pilot is maneuvering the airplane. This type of roll damper gain, high when stability is important and low when maneuverability is desired, is achieved with a nonlinear roll damper of the type installed in the F-8 airplane. The configurations of the nonlinear gain investigated during this study are depicted in Fig. 8. The roll damper computer diagram is presented as Fig. 9.



### C. FLIGHT PATH GEOMETRY

The flight path geometry is based on an analysis of what the pilot sees through the windscreen of the F-8 airplane while making an approach to a carrier landing.

First, the conditions necessary for the optimum carrier approach should be specified. In the most general terms, a constant airspeed should be maintained, with glide slope flown so as to keep the meatball of the Fresnel Lens Optical Landing System (FLOLS) "split" by the datum lights while the line-up of the airplane flight path is constantly coincident with the vertical plane containing the deck centerline.

With the foregoing in mind, the particular approach considered herein, is the one described by a  $4^{\circ}$  relative glide slope flown at an approach speed of 139 knots true airspeed. In actual practice, the F-8 pilot would fly the optimum angle of attack during the approach. At the airplane weight considered in this study, this optimum angle of attack results in a true airspeed of 139 knots. Fig. 10 depicts the vector diagram of the approach. The ship's speed through the water ( $U_S$ ), together with the ambient or natural wind (AW), sum up to the total wind over the deck (WOD) when the ship is headed into the wind. The relative glide path is the  $4^{\circ}$  path shown. The actual glide path angle ( $\gamma^*$ ) is seen to be a function of ship's forward speed and not ambient wind. Variations in ambient wind would change the airplane attitude, power required and relative speed, but not the angle of attack so long as desired airspeed is maintained. The more the ambient wind, the higher is the nose attitude required to maintain the same inertial path and angle of attack. The



relative speed, or the engaging speed, is approximately the difference between 139 knots and the wind over the deck. Sinking speed for this approach is the same regardless of ambient wind or ship's speed.

Fig. 11 shows the details of the relative path flown during the carrier approach maneuver. Dimensions shown are approximate for a typical U.S. Navy Attack Carrier. Visualization of the approach geometry is simplified if the flight path is considered to be traversed by the pilot's eye, as seen in Fig. 11. A  $4^\circ$  relative glide path would require an apparent "eye touch down point" 362 feet down the deck from the approach end of the deck. The approach end of the deck hereinafter will be called the "ramp." The deck landing area is 665 feet in length. Range (R) is defined as the horizontal distance from the ramp to the pilot's eye. The angles  $\eta_1$  and  $\eta_2$  are the angles between the apparent eye touch down point and the far edge of the flight deck and ramp, respectively. The distance  $h_0$  is the vertical height from the ramp to the pilot's eye when  $R = 0$ . When the pilot is precisely on the glide slope,  $h_0 = 25.3$  feet for the F-8 airplane in the approach configuration, as stated in Ref. 3.

It can be seen from Fig. 11 that equations which define the angles  $\eta_1$  and  $\eta_2$  as functions of range are:

$$\tan(4^\circ - \eta_1) = \frac{(R + 362)\tan 4^\circ}{R + 665} \quad (18)$$

and

$$\tan(4^\circ + \eta_2) = \frac{(R + 362)\tan 4^\circ}{R} \quad (19)$$



Two other degrees of freedom, or the visualization resulting from these degrees of freedom, are also functions of range. These are the altitude indication, observed from the FLOLS, and the lateral displacement from the deck centerline.

When the pilot is flying on the glide slope, the meatball appears to be "split" by the datum lights of the FLOLS. When above glide slope, the meatball appears above the datum lights and when flying below the glide slope the meatball is below the datum lights. Fig. 12 is a sketch of the Fresnel lens geometry as related to the pilot visualizations during the approach. Lens construction is such that the meatball virtual image is located 150 feet behind the lens box which is approximately four feet in total height. It can be seen here that meatball position on the lens unit delineates a glide slope angle to the viewer. Due to this angle definition feature, a large  $\Delta h$  at far range would place the meatball in the same position on the lens unit as would some smaller  $\Delta h$  at closer range. This simply means that the FLOLS is more sensitive as the pilot approaches it. From Fig. 12 it is seen that:

$$\frac{\Delta h'}{\Delta h} = \frac{150}{R + 362 + 150} \quad (20)$$

where  $\Delta h'$  is the distance in feet that the meatball is above the datum lights on the lens unit, and  $\Delta h$  is the distance in feet that the pilot's eye is above the desired glide slope.

Lateral displacement, as seen by the pilot, is a visualization of some reference point on deck located to one side of the centerline of the wind-screen (for  $\psi = 0$ ) with the deck centerline always pointing toward the same vanishing point on the horizon. The vanishing point effect here is emphasized to distinguish the lateral displacement visualization from the yaw visualization.



Fig. 13 shows, in a view above, the geometry of the lateral displacement visualization. The distance  $d$  is the actual lateral displacement in feet. The pilot views the apparent eye touch down point (selected as the reference point on deck) off to the side at an angle  $\eta_3$ . It can be seen that, for a given lateral displacement,  $\eta_3$  varies as a function of range, in accordance with:

$$\eta_3 = \tan^{-1} \frac{d}{R + 362} \quad (21)$$

The additional three degrees of freedom which are to be considered for the display are airplane pitch, yaw and roll. The visualization is simply an angular displacement of the field of view to correspond with the angle of pitch, yaw or roll. There is no variation with range for these angular perturbations. Fig. 14 is a sketch to aid in the visualization of yaw. It is a view from above and will be used in the next section to explain the details of the simulator display.

#### D. CARRIER APPROACH SIMULATOR DISPLAY

The display which simulates the pilot's view during the carrier approach maneuver consists of traces on an eight by ten centimeter screen of the cathode ray oscilloscope. Prior to a detailed description of the display, it is briefly stated that the display consists of a horizon trace, deck centerline and ramp traces, and a dot to represent the meatball of the FLOIS. Fig. 15 shows four sketches of the Carrier Approach Simulator Display. A main feature of the display is that the varying size of the traces of the carrier deck represents apparent growth of the deck as range decreases. The deck traces grow from very small to large in a nonlinear



manner in 28 seconds; this is the time required to fly the glide slope from a range of 5000 feet to the ramp at a relative speed of 105 knots. The display is viewed by the pilot making the simulated carrier approach while controlling the airplane with the control stick and rudder pedals.

Fig. 15A is the display for the on glide slope flight condition at a far distant range, with no yaw, lateral displacement, roll or pitch. The meatball is on the horizon and the deck centerline and ramp traces appear small in size and are geometrically located straight ahead in the field of view.

Fig. 15B shows the airplane to be above glide slope (meatball above horizon) and at closer range than in Fig. 15A. Also seen on Fig. 15B are the indications of nose down pitch and lateral displacement of the airplane to the left of the deck centerline. Lateral displacement is seen here as the deck centerline not perpendicular to the horizon. An angle other than 90 degrees between centerline and both horizon and ramp is apparent when laterally displaced. Pitch is seen simply as the complete display on the screen moved up to indicate nose down pitch of the airplane.

Fig. 15C indicates the below glide slope and right wing down flight condition. Pitch perturbation is zero. The range is approximately the same as that in Fig. 15B.

Fig. 15D shows that the approaching airplane is on glide slope, yawed nose left and at the closest range shown in any view. There is no lateral displacement seen in Fig. 15D since the deck centerline is perpendicular to the horizon.



Determination of dimensions and locations of the traces on the simulator display required that some actual viewing angles through the F-8 front wind screen be known. Fig. 16 shows the viewing angle possible through the F-8 front wind screen as obtained from the interpretation of photographs and actual measurements. It was estimated that the viewing angle in the vertical plane is 17.5 degrees; 8.5 degrees above the horizon and nine degrees below the horizon for the airplane attitude for this simulated approach. The above data locates the horizon and the apparent eye touch down point on the centerline trace of the display. They are points (1) and (2) respectively on Fig. 16. For the case of no perturbations or lateral displacements from centerline, the two points should remain fixed while the traces representing the deck centerline and ramp would lengthen with the decrease in range as the simulated approach is accomplished. Since the eight centimeter height of the display screen represents the 17.5 degree viewing angle, it can be stated that the ratio  $8/17.5$  is the display scale factor (SF) in centimeters per degree. It can be seen on Fig. 16 that point (1) should be located  $(SF) \times 9^{\circ} = 4.11$  centimeters from the bottom of the display screen. Location of point (2) should be  $(SF) \times 4^{\circ} = 1.83$  centimeters below the horizon, or point (1). The F-8 airplane roll axis was found to project 2.5 degrees above the horizon for the airplane attitude considered. For simplicity, the roll axis was assumed to pass through the pilot's eye and extend out at this angle. Point (3) on Fig. 16, therefore, identifies the position about which the display rotates to show airplane roll. This point is  $(SF) \times 2.5 = 1.14$  centimeters above the horizon.



The deck centerline length apparent on the display is the distance  $l_1$  plus  $l_2$  as seen in Fig. 16. These lengths may be calculated from:

$$l_1 = (SF)\eta_1 \quad (22)$$

and

$$l_2 = (SF)\eta_2 \quad (23)$$

where  $\eta_1$  and  $\eta_2$  are in degrees and are calculated for given values of range from equations (18) and (19). Equations (19) and (23) appear somewhat difficult to use, at first glance, since the right hand side denominator of the equations approaches zero as the pilot approaches the ramp. This problem is solved by virtue of the fact that, as the pilot nears the ramp during the approach, the ramp at some value of range, disappears from sight under the nose of the airplane. The disappearance of the ramp from sight in the actual approach would correspond to the ramp trace going off the bottom of the scope during the simulated approach. This allows easy simulation of the apparent deck centerline "growth" as range decreases. From Fig. 16 it is clearly seen that when  $\eta_2 = 5^\circ$  the ramp should just disappear off the bottom of the display. This corresponds to a range of 290 feet, from a solution of equation (19). The simulated approach could be continued for several seconds after the loss from sight of the ramp with no detrimental loss of features on the display or acuity of control.

As stated earlier, a dot on the display represents the meatball of the Fresnel Lens Optical Landing System (FLOLS). The on-glide-slope condition places the meatball at the horizon. Fig. 12 shows that the angle



$\eta_4$  is the angle seen by the pilot between the datum lights and the meatball. This angle is used to obtain correct placement of the meatball above the horizon on the display which will correspond to the pilot's eye being  $\Delta h$  feet above desired glide slope. Using the same tack as previously followed:

$$\eta_4 = \frac{\Delta h'}{R + 362} \quad (24)$$

and

$$u_2 = (SF)\eta_4(57.3) \quad (25)$$

where  $u_2$ , in centimeters, is the distance on the display that the meatball should be displaced above the horizon to correspond with  $\eta_4$ . The angle  $\eta_4$  is a function of  $\Delta h'$  and  $R$  from equation (24) and  $\Delta h'$  is a function of  $\Delta h$  and  $R$  from equation (20). After substitutions and simplification, it was found that:

$$u_2 = \frac{3920 \Delta h}{(R + 512)(R + 362)} \quad (26)$$

At the ramp, during an actual approach, the pilot sees the meatball disappear off the top or bottom of the FLOLS when he is 7.35 feet above or below glide slope, respectively. This would be seen as only .155 centimeters on the display from a solution of equation (26). Since this is considered too trivial an indication of a very serious flight condition, the simulator visualization used was that described by the equation:

$$u_2 = \frac{49.3 \Delta h}{(R + 362)} \quad (27)$$

which requires that  $u_2 = 1.0$  centimeter for  $\Delta h = 7.35$  feet at  $R = 0$ . This approximation still relates the realistic quality of a more sensitive meatball as range decreases.



Lateral displacement from the deck centerline is a visualization easily identified on the display as the deck centerline not perpendicular to the horizon. From Fig. 13, it can be seen that, for small displacements:

$$\eta_3 = \frac{d}{R + 362} \quad (28)$$

where  $d$  is the actual displacement in feet which is to be simulated on the display. The dimension on the display ( $u_1$ ) to simulate this displacement is obtained, using a similar course as previously followed:

$$u_1 = (SF)\eta_3 \quad (29)$$

or

$$u_1 = 25.9 \frac{d}{R + 362} \quad (30)$$

where  $u_1$  is the distance in centimeters that the apparent eye touch down point is displaced from the center of the screen to correspond with  $d$  feet actual displacement at a range ( $R$ ).

The effectiveness of the display depends to a great extent on the function of range as described in this section. The display dimensions ( $l_1 + l_2$ ) and ( $1.83 - l_1$ ) are the complete deck centerline length and the distance from horizon to the far edge of the deck, respectively. These two dimensions, together with the function

$$f(R) = \frac{\text{constant}}{R + 362}$$

are listed in Table V for various values of  $R$ . It can be seen from equations (27) and (30) that this latter function of range is that required



for the desired display effects for meatball sensitivity and lateral displacement, respectively. The three functions of range are set on function generators, scaled down or combined as appropriate, and sent as signals on trunk lines to the TR-48 computer or servo multipliers, as detailed in Fig. 17 and shown in simplified form in Fig. 2. The remaining electronic circuitry required to produce the actual display traces was developed by Princeton University Instrumentation personnel.

#### E. SIMULATED ATMOSPHERIC TURBULENCE

In order to increase the piloting task and evaluate the different roll damper gain configurations, atmospheric turbulence, in the form of gusts, was introduced as forcing functions in the airplane equations of motion. The gust spectrum was obtained by passing white noise obtained from a Gaussian noise generator through a first order filter with the transfer function (Ref. 4):

$$\frac{1}{\frac{s}{.314} + 1} \tag{31}$$

This gust spectrum is similar to the spectrum used in Ref. 5. A thirty minute long magnetic tape recording of the gust signal was made. Random portions of the tape recording were used during all flights in the simulator. The root mean square (RMS) level of the atmospheric turbulence about a zero mean lateral wind was changed during different portions of the investigation. These various RMS levels are tabulated in Table VI.

In the development of the longitudinal equations of motion, it was assumed that the airplane's forward velocity was held constant, and the drag equation was omitted. In keeping with this simplified set of longitudinal equations, it was felt that the addition of turbulence in the



airplane's forward velocity would not add materially to the lateral-directional handling qualities study. Therefore, no gusts parallel with flight path were added to the longitudinal equations of motion.

Initial investigation of the piloting task was conducted with atmospheric turbulence composed of both vertical and lateral gusts causing perturbations in angle of attack and sideslip angle, respectively, in the equations of motion. Perturbations in angle of attack and sideslip angle due to gusts were:

$$\alpha_g = \frac{w_g}{V_0} \quad (32)$$

and

$$\beta_g = \frac{v_g}{V_0} \quad (33)$$

During this initial investigation it became apparent that the introduction of  $\alpha_g$  type gusts increased the piloting task to the point where it greatly detracted from the lateral-directional handling qualities investigation. This occurred with even low levels of atmospheric turbulence. The derogatory effect of the  $\alpha_g$  gusts may be partially attributed to the simplified set of longitudinal equations chosen for the simulation. In addition, the present development of the simulator furnishes no angle of attack or normal acceleration information to the pilot. It was felt that the simplification afforded by these assumptions in the longitudinal equations of motion was in keeping with the purpose of this study. It must be noted that, during the usual lateral control stick motions made by the pilot, the pilot introduces small elevator deflections which perturbed the simulator in both pitch angle and angle of attack. These



inadvertent elevator deflections made the longitudinal piloting task sufficiently difficult for the purpose of this investigation. It was therefore necessary to introduce only lateral gusts in the equations of motion.

As indicated previously, lateral gusts effectively take the form of forcing functions in the airplane's equations of motion. Since the airplane's response to these gust perturbations are dependent on the airplane stability derivatives, the gusts were introduced by substituting  $(\beta + \beta_g)$  for  $\beta$  in the lateral-directional equations of motion [equations (3), (4), and (5)]. The introduction of the gust into the equations of motion on the analog computer may be seen in Fig. 4. It will be noted that no attempt was made to account for gust wave length or gradients in the gust model employed, as it was assumed that gusts encompassed the entire airplane equally. Both Ref. 5 and Ref. 6 indicated the validity of the gust model chosen. It is interesting to note that the pilots who flew the simulator during the investigation felt that the atmospheric turbulence was realistic in the manner in which the airplane responded to the gusts, as seen on the display.



### III. FLIGHT EXPERIMENTS

#### A. PROCEDURES

The procedures adopted for the first phase of this study were aimed at an evaluation of the carrier approach simulator itself. It was thought that more credence could be attached to any data resulting from the use of the simulator if it could be shown that flight in the simulator had some non-trivial correspondence with flight in an actual airplane.

The task chosen for the evaluation was the flying of simulated carrier approaches by four pilots, each flying four selected airplane configurations. The four airplane configurations were for hypothetical airplanes with neither roll nor yaw damper systems. They were chosen because actual field carrier\* flight information, in the form of Cooper ratings, were available from Ref. 7. The object was to determine whether carrier approaches on the simulator merited corresponding Cooper ratings as did the field carrier landing approaches made by other experienced pilots who flew nearly identical configurations in a variable stability airplane. The dimensional stability derivatives which describe the four airplane configurations from Ref. 7 are reproduced in Table IV. All approaches in this simulator evaluation phase were flown in "light" turbulence. The adjective descriptions of light, moderate and severe atmospheric turbulence are defined in Table VI.

The pilot was allowed to fly each configuration until he felt he was familiar with its handling qualities. After this familiarization period a

---

\*Carrier landings practiced at an airfield



minimum of eight approaches were flown for performance recording. Pilot-airplane performance was measured quantitatively by recording time histories of vertical displacement from the glide slope and the lateral displacement from the carrier deck centerline. These data were tabulated for the termination of the simulated approach, i.e. at the ramp. Also recorded were the Cooper rating and any comments or remarks by the pilot concerning his flight in that configuration. Approximately 150 approaches were flown and recorded in this phase, in addition to the familiarization approaches.

The second phase of this study consisted of the investigation of four different configurations of a non-linear roll damper for the F-8 airplane in the carrier approach maneuver (Fig. 8). The procedures consisted of flying for performance recording a minimum of eight approaches by each of six pilots with each different roll damper configuration. Prior to flying the recorded approaches the pilot was allowed to fly each configuration until he was familiar with its handling qualities. These approaches were flown in the presence of both "moderate" and "severe" atmospheric turbulence.

As before, performance was measured quantitatively by recording time histories of vertical displacement from the glide slope and lateral displacement from the centerline. Data were tabulated for the terminal point of the simulated approach. Also recorded were the pilots Cooper rating and comments at the conclusion of flying each F-8 roll damper configuration. More than 400 simulated approaches were flown and recorded in this phase of the study in addition to the familiarization approaches.



During the flights in the simulator the pilots were told only that they were flying different airplane configurations in the first phase, and different roll damper configurations in the second phase. The pilot was not told what configuration he was flying. The order in which the different configurations were flown by each pilot was arbitrary. Some of the pilots flew the same configurations more than once during his evaluation period. It is worthy of note that, in most of these cases, the pilots repeated their initial evaluation of the configuration they reflew.

#### B. EVALUATION OF THE FLIGHT SIMULATOR

The six degrees of freedom simulator developed in this study was intended primarily as a tool for investigating flight control systems, and possibly for the investigation of instrument approach displays. The use of the simulator for instrument approach display investigation was not a direct part of this study.

In order to determine how results from simulator studies might be expected to compare with similar studies conducted in actual airplanes, the four hypothetical airplane configurations from Ref. 7 were chosen to be "flown" on the simulator. The configuration numbers are those from Ref. 7. The use of the configurations from Ref. 7 was considered to be a reasonable "yardstick" for two reasons: first, the pilot task in the actual flights of Ref. 7 was a field carrier approach and second, the object of the study in Ref. 7 was lateral-directional handling qualities. The basis of the present study was the comparison of pilot opinion ratings (Cooper ratings) between similar airplane configurations flown in the simulator and in the variable stability airplane of Ref. 7. In both this



study and in Ref. 7 a minimum of emphasis was placed on the longitudinal handling qualities of the airplane.

The results of the simulator flights are tabulated in Table VII. Also listed in Table VII are the average Cooper ratings determined from the actual flight tests of the four configurations from Ref. 7. The results listed in Table VII indicated that, in general, the simulator is capable of reproducing actual flight data to a reasonable degree. One very noticeable point in Table VII is the fact that all four of the pilots engaged in the simulated flights rated the four configurations in the same order, from best to worst. It may also be noticed that the different pilots, with very few exceptions, rated each configuration nearly the same. Comparing the average Cooper ratings from the simulator flights with the results of Ref. 7, it is very apparent that major changes in airplane configurations are readily discernable in the simulator. This is most apparent in the results of configurations six and 20, the best and worst configurations respectively. In configuration six, the average Cooper ratings from the simulator (2.8) and the actual flight tests (2.6) are nearly identical. In configuration 20, the average Cooper rating from the simulator (5.4) is somewhat better than that found in actual flight tests (6.5), although two of the four simulator pilots rated the configuration as a six. These high Cooper ratings indicate unacceptable airplane configurations, yet it was felt that the better rating was found in the simulator since the pilot does not feel that he is personally in danger in the simulator, as he might feel in an actual flight situation.



It is also apparent from the comparison of the results of the simulator flights in configurations 7 and 17, that all four pilots who flew the simulator reversed the relative Cooper ratings of these two configurations with respect to the results of Ref. 7. A comparison of the Cooper ratings of configurations 7 and 17 individually with their respective Cooper ratings from Ref. 7, indicates reasonable correlation between the simulator and actual flight data. The fact that the relative standings of configurations 7 and 17 were reversed with respect to Ref. 7 is not considered too serious since these two configurations were rated quite closely in both the simulator and in actual flight. The consistent reversal of the relative standings of these two configurations does however, indicate that the simulator possibly lacks some motion cue which is necessary to properly differentiate between the two configurations. Examination of the dimensional stability derivatives which describe these two configurations (Table IV) indicates that the major differences between the two configurations are in their yawing derivatives ( $N_{\delta_a}$ ,  $N_p$ ,  $N_r$ ). Configuration 17 exhibits proverse aileron yaw ( $N_{\delta_a}$ ), positive yaw due to roll rate ( $N_p$ ), and lower yaw damping ( $N_r$ ) than configuration 7 in which  $N_{\delta_a}$  and  $N_p$  are zero. Further, it was noted in the pilot's comments that yaw was the most bothersome problem encountered in configuration 17 and was the basis for the poorer Cooper ratings. The pilots generally felt that it was more difficult to control configuration 17's yawing motions. Since it is impossible to see sideslip on the simulator display, it was felt that the simulator did not present the cues necessary to effectively control sideslip. This seems to indicate that the simulator should have a visual presentation similar to



the "ball" portion of an airplane's turn indicator. The addition of the sideslip indicator should give the pilot the information required to effectively coordinate the aileron and rudder controls. In the variable stability airplane of Ref. 7, the pilot had a turn indicator as well as the physical cues of sideslip. This may have made it possible for the pilots to control configuration 17 more easily in the variable stability airplane. The lack of these cues in the simulator may possibly explain why the relative Cooper ratings from the simulator study of configurations 7 and 17 were reversed with respect of results of Ref. 7.

Another important aspect of the simulator evaluation involves the observation of a correlation of the measured pilot-airplane performance to the Cooper ratings assigned by pilots. Figure 18 is a plot of vertical displacement from the glide slope and lateral displacement from the deck centerline as functions of Cooper rating. The shaded areas encompass approximately 88% of the data representing these displacements as functions of Cooper ratings. The straight lines represent the best straight line approximation to the average data plotted in these areas. It seems apparent in Figure 18 that the better Cooper ratings were assigned to those configurations which had better pilot-airplane performance in lateral displacement. The poorer Cooper ratings were given when the performance in lateral displacement indicated poorer lateral-directional handling qualities. This trend is considered to be one aspect attesting to the realism of the simulation. It also seems apparent in Figure 18 that the vertical displacement from the glide slope is nearly independent of Cooper rating. This may also be considered as further verification of



the simulation since the longitudinal dynamics of all airplane configurations were the same, the longitudinal stability derivatives were not changed between configurations. It may be noted in Table VII that nearly every pilot exhibited some deviation from the above mentioned trends, but the average values from each configuration followed the indicated trends.

Comments, remarks, and observations of the investigators and the pilots who flew the simulator in this evaluation phase were also considered noteworthy, but somewhat less important than measured performance and Cooper rating data. It was observed that all pilots took between one and two hours to "learn" to fly the simulator. One fact considered important is that the most experienced carrier pilot, Pilot F, a graduate of the Navy test pilots school, learned to fly the simulator with precision most rapidly. Pilot D had difficulty learning to correct for nose attitude with respect to the visualization of the horizon on the display. Pilot E had difficulty with wing attitude but not with nose attitude. This latter pilot, at first, tended to increase the bank angle when the intended correction was to level the wings. This latter pilot was the most experienced instrument pilot. His wing attitude learning problem is difficult to explain since the display has the same visual cue for wing attitude as does an aircraft gyro horizon. Each visual cue has the horizon rotating in the same manner with respect to the viewer. The nose attitude and wing attitude learning problems seemed to be overcome when these individuals were able to figuratively place themselves in a cockpit looking out at the carrier deck and horizon.



During the evaluation of the simulator it became apparent that a number of possible improvements might be made to the simulator. The first of these was indicated by the difficulty some of the pilots encountered in learning to fly the simulator. It was felt that the addition of a "hood" which restricts the pilots view to just the display and the interior of the simulator might make the learning problem easier. The hood should help the pilot place himself figuratively in an airplane which is moving, rather than having him see the display move with respect to his fixed surroundings. Another improvement would be the use of a display screen larger than the eight by ten centimeter display employed during this study. This would tend to make the viewing angles of the display the same as the viewing angles in the actual airplane.

Two possible additions to the simulator, which may be necessary if the simulator is to be used for longitudinal studies, would be an angle of attack indicator and a pilot controlled throttle. It is also possible that the addition of an angle of attack indicator would be beneficial without the addition of the throttle.

Two of the three experienced jet pilots who flew the simulator indicated that the simulator stick forces were somewhat lighter than those in the F-8 airplane. Although these pilots did not feel that this detracted from the study being conducted, they did feel that more realistic stick forces would enhance the simulator. It must be noted that all the pilots felt that the display was effective and realistic in the manner in which it presented the flight information.



This, along with the fact that none of the pilots felt that any necessary flight information was missing, seemed to validate the simulator display.

It was felt that the simulator, or modification thereto, should prove to be a useful experimental tool for evaluating differences in control systems.

### C. NONLINEAR ROLL DAMPER INVESTIGATION

The nonlinear roll damper considered in this investigation is one in which roll rate is fed back to the ailerons with a variable gain ( $K_p$ ). The feedback gain is a function of lateral control stick deflection. The four configurations of the nonlinear gain investigated are depicted in Fig. 8.

During this investigation the minimum and maximum magnitudes of  $K_p$  were held constant at the values presently in use on the F-8 airplane: 0.025 and 0.685, respectively. This decision was supported by an investigation of the airplane's response to pulse inputs of rudder and aileron, which indicated no appreciable differences in the airplane's response for values of  $K_p$  between 0.5 and 0.8.

With the maximum and minimum values of  $K_p$  thus eliminated as parameters, the investigation was restricted to an attempt to determine the effects of the two remaining characteristics necessary to define the roll damper gain function. These are the width of a "flat top" and the slope of the sides.

The basic theme used in selecting the roll damper gain functions, was that of providing the pilot with more damping over a wider range of stick deflections than is available in the current F-8 airplane. This added damping, of course, is gained at the expense of the pilot's roll rate



command authority. The roll damper gain function presently employed on the F-8 airplane is configuration 1 in Fig. 8. The additional shapes investigated were defined by varying only one of the two parameters with respect to configuration 1. Thus, the two configurations which had a finite width to the "flat top" had the same slope to the sides as configuration 1, and the configuration which had a different slope to the sides had a pointed top.

The four configurations were flown by each of six pilots in two atmospheric turbulence conditions. Tables VIII and IX show the results of these simulated carrier approaches for the moderate and severe turbulence conditions, respectively. Listed on these tables are the pilot's Cooper ratings and the average terminal values of deviation from the glide slope and lateral displacement from the deck centerline, for each configuration. Two typical time histories of simulated approaches are shown in Figs. 19 and 20. In these figures the starting point for the simulated approach is at the left margin and the termination of the approach is at the right margin of these graphs. These left and right margins correspond respectively to the beginning of the approach at a range of 5000 feet, and the termination of the approach over the ramp. The terminal values of altitude deviation from the glide slope (channel one) and lateral displacement from the deck centerline (channel six) were obtained from such time histories. Time histories were recorded for all the simulated approaches in the nonlinear roll damper investigation.

Examination of the results shown in Table VIII (moderate atmospheric turbulence) reveals that the Cooper ratings given by the pilots followed no set pattern. The averages of Cooper ratings for each configuration shown in



Table VIII are only spread between 2.7 and 3.1. Individual ratings in these moderate turbulence flights have no apparent correlation with airplane-pilot performance. In no case did a pilot assign the best Cooper rating to that configuration which he flew most precisely in both altitude and lateral displacement. In the most extreme case, pilot A gave the worst Cooper rating to that configuration with which he performed most precisely in both altitude and lateral displacement. It would appear at this point that either the turbulence level was too low or the configurations were not distinctive enough to yield clear comparisons. It will be shown later that a preferred configuration did clearly emerge in the higher atmospheric turbulence flight condition. Therefore, it is concluded that this turbulence level was too low to show meaningful differences. It is believed that the moderate atmospheric turbulence level limited the required lateral control stick activity to a degree where the pilots were unable to distinguish differences in the nonlinear roll damper configurations tested.

Simulated carrier approaches at the severe atmospheric turbulence level, on the other hand, produced some meaningful results. It can be seen in Table IX that roll damper configuration 1 received the best Cooper rating and was flown with less lateral displacement error than all others. The altitude deviation data shows no correlation between Cooper rating and altitude deviation from glide slope. This is believed to be the result of the unchanged longitudinal airplane dynamics, and was also apparent in the phase of this thesis concerned with the simulator evaluation.



Roll damper configurations 2, 3, and 4 were rated about equally in severe atmospheric turbulence, with no clear distinction concerning their relative merits. A plot of the averaged data for each configuration, at both atmospheric turbulence levels, falls in the bands defined in Fig. 18. However, the datum points which make up these average points are so widely scattered that no inferences will be drawn in this regard. The only conclusions considered valid in the roll damper investigation are that, in moderate atmospheric turbulence the pilots had no strong preference as to the roll damper configuration, and that in severe atmospheric turbulence they clearly prefer configuration 1. It should be noted that configuration 1 is the nonlinearity currently used in the F-8 airplane's lateral control system.

There remains one suggestion which should be considered. It has been shown that configuration 1 was rated superiorly to the other three configurations considered in this investigation. Examination of the four configurations indicates that, if there is an optimum configuration other than configuration 1, it is likely to be one which has a steeper slope to the sides. The steeper slope would give the pilot more lateral maneuverability for small stick deflections and still afford good damping with no stick deflection. With the steeper slope to the sides, a "flat top" may possibly be advantageous. A study directed along these suggested lines is considered worthy of some future effort.

The use of different levels of atmospheric turbulence, while not a main part of this study, did yield some information which is worthy of mention. It has been stated that flight information obtained in "moderate"



turbulence on the simulator showed no clear pilot preferences for any one roll damper configuration. Simulated flights in "severe" turbulence, however, allowed differences to become apparent to the pilots. This would indicate that future studies using the simulator should be conducted only in severe turbulence to aid in making evident the differences in control system parameters.



#### IV. CONCLUSIONS AND RECOMMENDATIONS

The phase of this study concerned with the development and evaluation of the flight simulator lead to the following conclusions.

1. The simulator display was found to be effective and realistic in the manner in which it presents the flight information. This display may be modified to suit the purposes of further investigations.

2. The flight simulator is capable of reproducing actual flight test information with meaningful correspondence, when there are non-trivial differences in the parameters under investigation. The flight simulator should prove to be a useful experimental tool.

3. There may be a direct correspondence between average pilot-airplane lateral-directional performance and pilot opinion rating (Cooper rating), when there are notable differences in the lateral-directional control systems being evaluated. This correspondence is strongly indicated for group average performance and opinion rating. Individual pilots will deviate from this pattern.

4. The changing of the simulated lateral-directional characteristics of the airplane does not effect pilot-airplane longitudinal performance when the simulated longitudinal dynamics are not changed.

Based on the results of the nonlinear roll damper investigation the following conclusions were drawn.

1. The pilot opinion ratings and pilot-airplane performance obtained from the simulator flights, in moderate atmospheric turbulence, indicated no preferred roll damper system of the four configurations tested.



2. The pilot opinion ratings and pilot-airplane performance in severe atmospheric turbulence, clearly indicated a preference for roll damper configuration one. No distinction is apparent between the remaining three roll damper configurations tested, in severe turbulence.

It is recommended that:

1. A visual presentation similar to the "ball" portion of an airplane's turn and bank indicator be added to the simulator display to give the pilot the information required to effectively coordinate the aileron and rudder controls.

2. An investigation be conducted concerning the possible improvement afforded by a "hood" for the display, a larger display screen, an angle of attack indicator and a pilot controlled throttle.

3. A simulator investigation be conducted to determine if a steeper slope to the sides of the nonlinear roll damper gain function, with or without a "flat top", is more advantageous than the configuration presently in use on the F-8 airplane (configuration 1).

4. Any future control system studies on this simulator be conducted in severe turbulence to aid in making evident the differences in parameters being studied.



REFERENCES

1. Cooper, George E.: Understanding and Interpreting Pilot Opinion. Institute of the Aeronautical Sciences, Preprint No. 683, (Presented at the 25th Annual Meeting January 28-31, 1957).
2. Seckel, Edward: Stability and Control of Airplanes and Helicopters, 1st ed., Academic Press, New York and London, 1964.
3. Anon: Aircraft Recovery Bulletin No. 61-12A Mark 6 Mods 0 and 1 Fresnel Lens Optical Landing Systems, NAEL-SE-431, 30 September 1963.
4. Seckel, E., Traybar, J.J., and Miller, G.E.: Longitudinal Handling Qualities for Hovering, Princeton University, Aeronautical Engineering Department Report No. 594, December 1961.
5. Durand, T.S., and Teper, G.L.: An Analysis of Terminal Flight Path Control in Carrier Landing, Systems Technology, Inc., Inglewood, California, Technical Report No. 137-1, August 1964.
6. Oldmixon, W.J.: The Acquisition, Reduction, and Analysis of Turbulence Data Associated With PA Configuration Approaches to Carrier Landings, Princeton University, Aeronautical Engineering Department Report No. 563, July 1963.
7. Seckel, E., Miller, G.E., and Nixon, W.B.: Lateral-Directional Flying Qualities, Power Approach, Princeton University, Aerospace and Mechanical Sciences Department Report No. 727, Unpublished.



Operating conditions	Adjective rating	Numerical rating	Description	Primary mission accomplished	Can be landed
Normal operation	Satisfactory	1	Excellent, includes optimum	Yes	Yes
		2	Good, pleasant to fly	Yes	Yes
		3	Satisfactory, but with some mildly unpleasant characteristics	Yes	Yes
Emergency operation	Unsatisfactory	4	Acceptable, but with unpleasant characteristics	Yes	Yes
		5	Unacceptable for normal operation	Doubtful	Yes
		6	Acceptable for emergency condition only*	Doubtful	Yes
No operation	Unacceptable	7	Unacceptable even for emergency condition*	No	Doubtful
		8	Unacceptable - dangerous	No	No
	9	Unacceptable - uncontrollable	No	No	
	10	Catastrophic	Motions possibly violent enough to prevent pilot escape	No	No

\*Failure of a stability augments

TABLE I. COOPER PILOT OPINION RATING SYSTEM



TABLE II

PILOT FLIGHT EXPERIENCE SUMMARY

Pilot A B.S. degree in Aeronautical Engineering.

Currently a candidate for the M.S.E. degree in Aeronautical Engineering. U.S. Navy pilot.

Total flight time	1650 hours
Total reciprocating time	1550 hours
Total jet time	100 hours
Total carrier landings	172

Pilot B B.S. degree in Aeronautical Engineering.

Currently a candidate for the M.S.E. degree in Aeronautical Engineering. U.S. Navy pilot.

Total flight time	2300 hours
Total reciprocating time	2300 hours
Limited jet experience	
Limited carrier experience	

Pilot C B.S. degree in Aeronautical Engineering.

Currently a candidate for the M.S.E. degree in Aeronautical Engineering. U.S. Navy pilot.

Total flight time	1650 hours
Total reciprocating time	300 hours
Total jet time	1350 hours
Total jet carrier landings	278

Pilot D M.S.E. degree in Aeronautical Engineering, research test pilot, U.S. Naval Reserve pilot.

Total flight time	2500 hours
Limited jet experience	
Limited carrier experience	

Pilot E Graduate of U.S. Naval Test Pilot School, Patuxent River, Maryland, U.S. Navy test pilot.

Total flight time	4800 hours
Total reciprocating time	3100 hours
Total jet time	1700 hours
Total F-8 time	250 hours
Total jet carrier landings	22



TABLE II (continued)

Pilot F Graduate Aeronautical Engineer, Graduate of U.S. Naval Test Pilot School, Patuxent River, Maryland, U.S. Navy test pilot.

Total flight time	2300 hours
Total reciprocating time	500 hours
Total jet time	1800 hours
Total jet carrier landings (F-8)	290



TABLE III  
F-8 AIRPLANE DATA

Physical:

$b$	= 35.7 feet
$C_{L_0}$	= 0.895
$\bar{c}$	= 11.8 feet
c.g. @	$24\% \bar{c}$
$I_{xx}$	= 10,200 slug-feet <sup>2</sup>
$I_{yy}$	= 96,000 slug-feet <sup>2</sup>
$I_{zz}$	= 101,200 slug-feet <sup>2</sup>
$S$	= 375 feet <sup>2</sup>
$V_0$	= 139 kts. = 235 feet/second
$W$	= 22,000 pounds
$\delta_a$	= $\pm$ 30 degrees
$\delta_e$	= +16 degrees -20 degrees
$\delta_r$	= $\pm$ 17 degrees
$\eta$	= 1.7 degree (angle between body and principal axis)

Aerodynamic derivatives:

longitudinal

$C_{L_\alpha}$	= +2.6 per radian
$C_{L_{\delta_e}}$	= +0.39 per radian
$C_{m_q}$	= -4.5 per radian/second
$C_{m_{\dot{\alpha}}}$	= -0.55 per radian/second
$C_{m_\alpha}$	= -0.38 per radian
$C_{m_{\delta_e}}$	= -0.84 per radian



TABLE III (continued)

lateral-directional

$C_{y\beta}$	= -1.26 per radian
$C_{yp}$	= +0.41 per radian/second
$C_{yr}$	= +0.28 per radian/second
$C_{y\delta_r}$	= +0.23 per radian
$C_{lp}$	= -0.276 per radian/second
$C_{lr}$	= +0.15 per radian/second
$C_{l\beta}$	= -0.187 per radian
$C_{l\delta_a}$	= +0.071 per radian
$C_{l\delta_r}$	= +0.01 per radian
$C_{nr}$	= -0.33 per radian/second
$C_{np}$	= -0.04 per radian/second
$C_{n\beta}$	= +0.246 per radian
$C_{n\delta_a}$	= -0.025 per radian
$C_{n\delta_r}$	= -0.124 per radian



TABLE IV

## AIRPLANE STABILITY DERIVATIVES FROM REFERENCE 7

Stability Derivative	Configuration Number From Reference 7			
	6	7	17	20
$L_p$	-3.83	-1.38	-1.52	-1.28
$L_\beta$	-16.0	-16.0	-15.8	-16.0
$L_r$	+1.75	+4.77	+3.46	+6.03
$N_p$	0	0	+0.40	+0.30
$N_\beta$	+2.56	+2.42	+2.673	+2.187
$N_r$	-0.281	-0.726	-0.586	-0.826
$N_{\delta_a}/L_{\delta_a}$	0	0	+0.025	+0.130
$Y_v$	-0.254	-0.254	-0.254	-0.254
$g/v_0$	+0.181	+0.181	+0.181	+0.181



TABLE V  
DISPLAY RANGE FUNCTIONS

Range ft.	Elapsed time sec.	$l_1 + l_2$ cm	$1.83 - l_1$ cm	$\frac{10^3}{R+362}$
5000	0	.183	1.74	.187
4500	2.82	.221	1.73	.206
4000	5.65	.251	1.72	.229
3500	8.47	.311	1.70	.259
3000	11.3	.366	1.68	.297
2500	14.1	.434	1.65	.349
2000	17.0	.525	1.63	.423
1500	19.8	.694	1.58	.537
1000	22.6	.978	1.51	.733
500	25.4	1.786	1.36	1.16
250	26.9	3.22	1.21	1.64
0	28.2		1.01	2.76



TABLE VI

## SIMULATED ATMOSPHERIC TURBULENCE

Gust Level	Adjective Level	RMS*	
		kts.	ft./sec.
1	light	4.1	6.8
1.5	moderate	6.2	10.2
3	severe	12.3	20.4

\*About zero mean lateral wind



	AIRPLANE CONFIGURATION NUMBER FROM REFERENCE 7											
	6			7			17			20		
	Cooper Rating	Displacement Vertical feet	Displacement Lateral feet	Cooper Rating	Displacement Vertical feet	Displacement Lateral feet	Cooper Rating	Displacement Vertical feet	Displacement Lateral feet	Cooper Rating	Displacement Vertical feet	Displacement Lateral feet
Pilot												
A	3.0	0.2	4.7	3.5	1.0	5.8	5.5	2.0	10.4	6.0	0.8	13.1
B	3.0	0.8	5.2	3.5	0.8	10.2	4.5	0.6	23.8	5.0	1.3	16.1
C	2.0	1.0	8.1	2.7	1.3	11.6	3.5	1.6	9.4	6.0	1.2	14.7
D	3.0	2.6	6.7	3.0	2.0	6.6	3.5	1.1	5.3	4.5	1.2	9.0
Average From Simulator	2.8	1.2	6.2	3.2	1.3	8.6	4.3	1.3	12.2	5.4	1.1	13.2
Average From Reference 7	2.6			4.3			3.5			6.5		

TABLE VII

RESULTS OF FLIGHT IN EVALUATION OF THE SIMULATOR



Pilot	ROLL DAMPER CONFIGURATION NUMBER											
	1			2			3			4		
	Cooper Rating	Displacement Vertical feet	Displacement Lateral feet	Cooper Rating	Displacement Vertical feet	Displacement Lateral feet	Cooper Rating	Displacement Vertical feet	Displacement Lateral feet	Cooper Rating	Displacement Vertical feet	Displacement Lateral feet
A	4.0	0.9	5.5				3.0	1.0	4.7	6.0	0.5	4.3
B	2.0	0.7	5.3	0.7	7.4		2.0	0.4	5.5	2.5	0.6	8.0
C	2.0	0.6	5.1	1.0	3.6		2.5	0.5	3.6	2.5	0.7	8.1
D	2.5	0.8	7.9	0.9	7.7		3.0	2.1	14.9	3.5	0.7	8.8
E	4.0	0.7	10.9	1.6	7.2		3.0	0.9	12.5	2.0	1.4	14.9
F	3.0	1.2	9.0	1.2	8.4		2.5	1.4	12.1	2.0	0.8	11.3
Average Values	2.9	0.8	7.3	1.1	6.9		2.7	1.0	8.9	3.1	0.8	9.2

TABLE VIII

RESULTS OF ROLL DAMPER CONFIGURATION EVALUATION

AT MODERATE TURBULENCE LEVEL



ROLL DAMPER CONFIGURATION NUMBER

Pilot	1			2			3			4		
	Cooper Rating	Displacement		Cooper Rating	Displacement		Cooper Rating	Displacement		Cooper Rating	Displacement	
		Vertical feet	Lateral feet									
A	7.0	0.9	2.5	7.0	1.2	6.2	6.0	1.2	6.4	6.5	1.5	8.2
B	3.3	1.1	8.1	3.5	1.1	9.3	4.0	1.1	9.1	2.5	0.9	4.2
C	2.7	0.9	6.6	4.0	1.0	9.0	3.0	0.9	9.8	2.5	0.7	6.2
D	3.0	1.1	8.4	3.0	1.0	7.7	5.0	0.9	8.2	4.0	1.1	8.4
E	3.0	1.1	8.8	4.0	0.9	20.2	3.0	1.8	11.4	5.0	2.4	18.2
F	2.5	1.4	11.6	3.0	1.0	15.9	5.0	1.8	15.8	4.0	1.9	20.7
Average Values	3.6	1.1	7.7	4.1	1.0	11.4	4.3	1.3	10.2	4.1	1.4	11.0

TABLE IX

RESULTS OF ROLL DAMPER CONFIGURATION EVALUATION

AT SEVERE TURBULENCE LEVEL



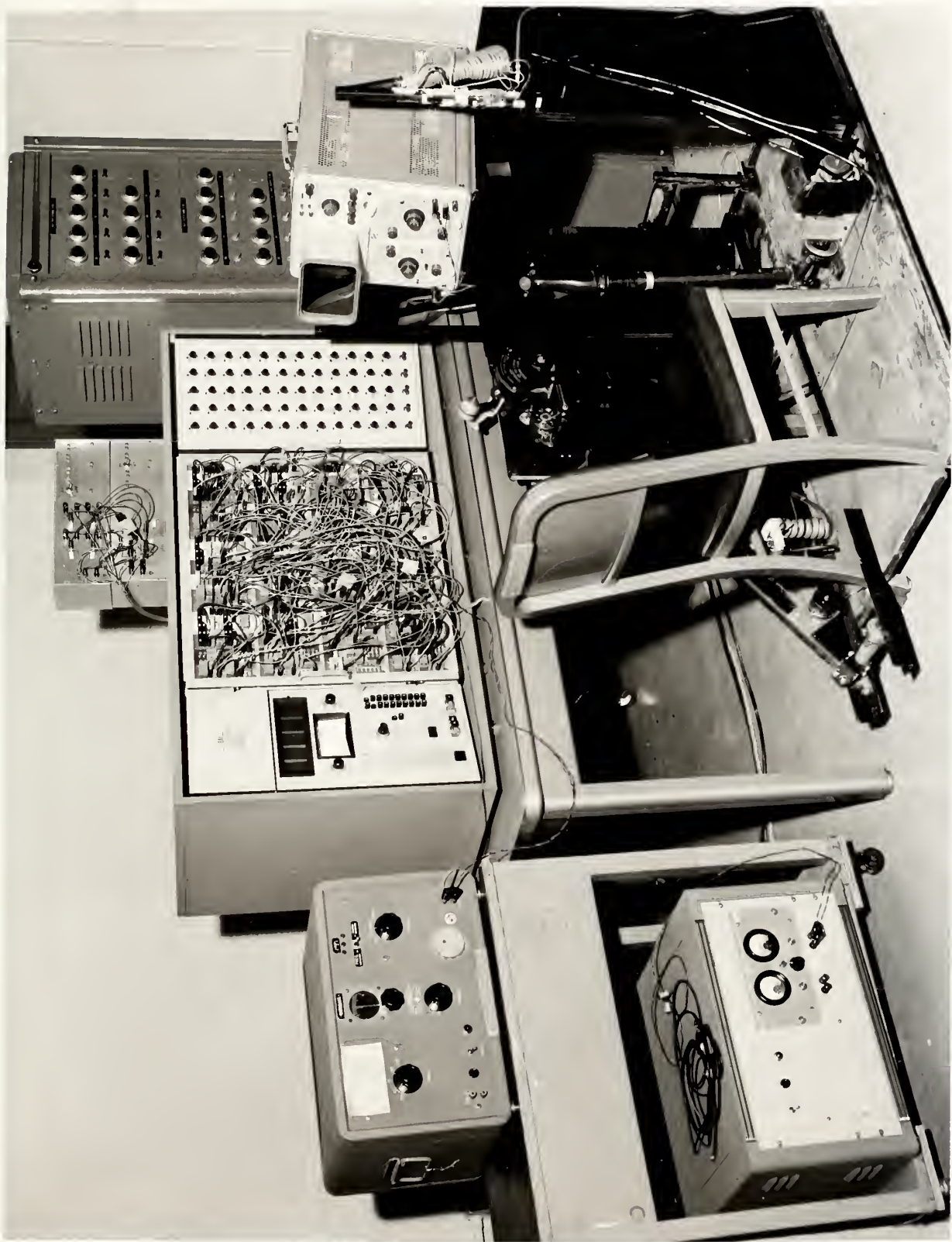


FIGURE 1  
CARRIER APPROACH SIMULATOR  
SET-UP



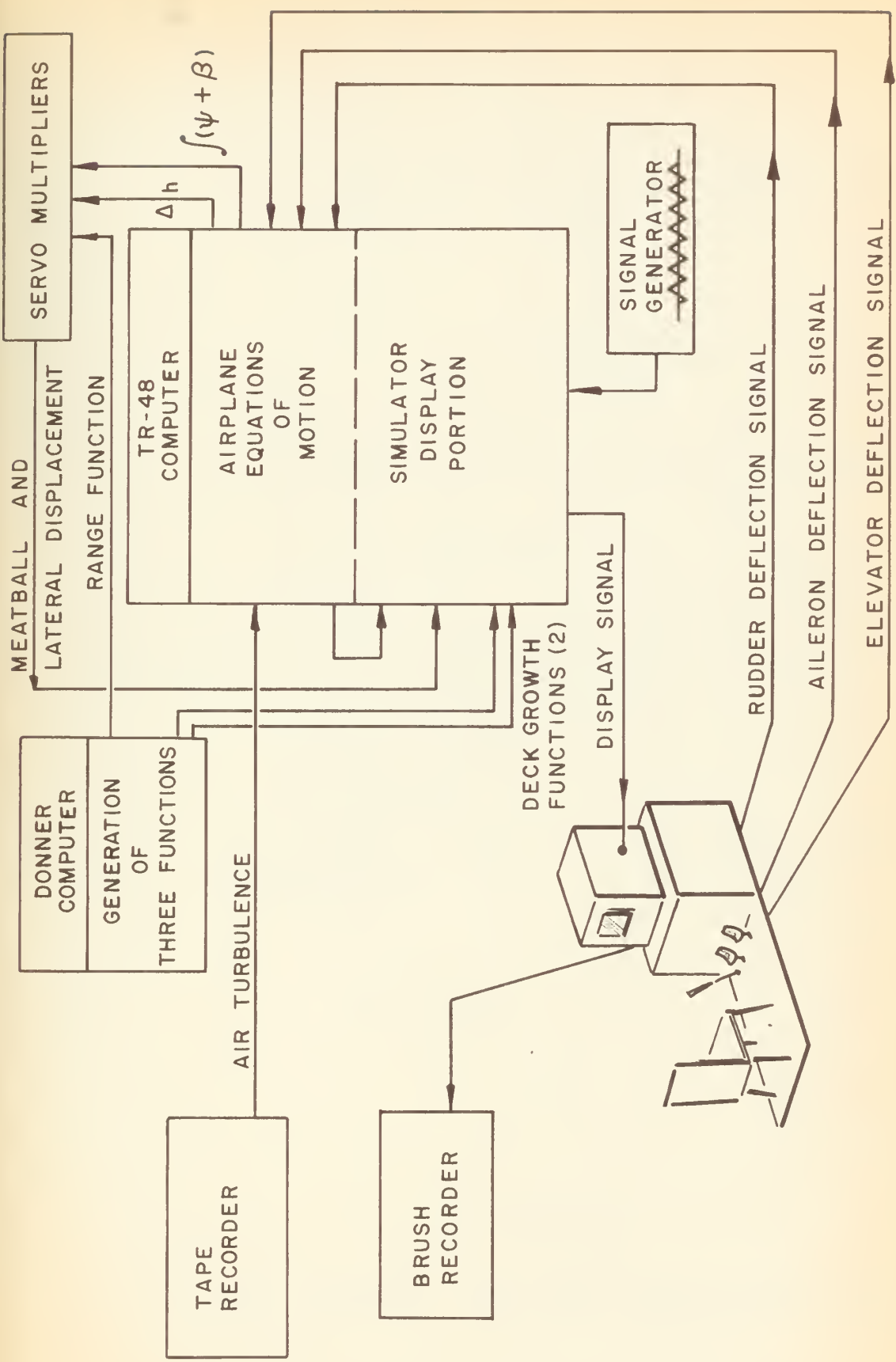


FIGURE 2  
 CARRIER APPROACH SIMULATOR FUNCTIONAL DIAGRAM



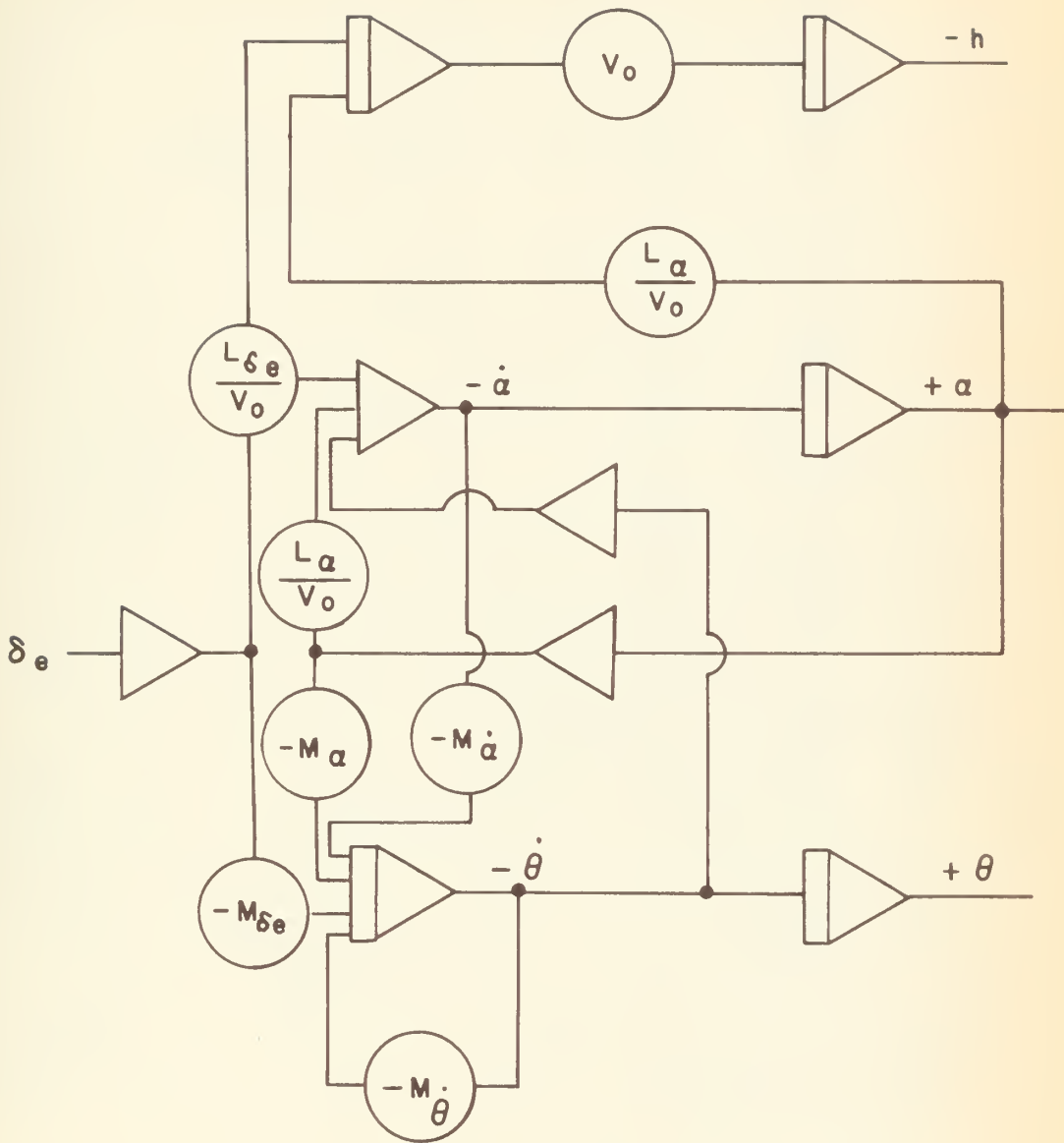


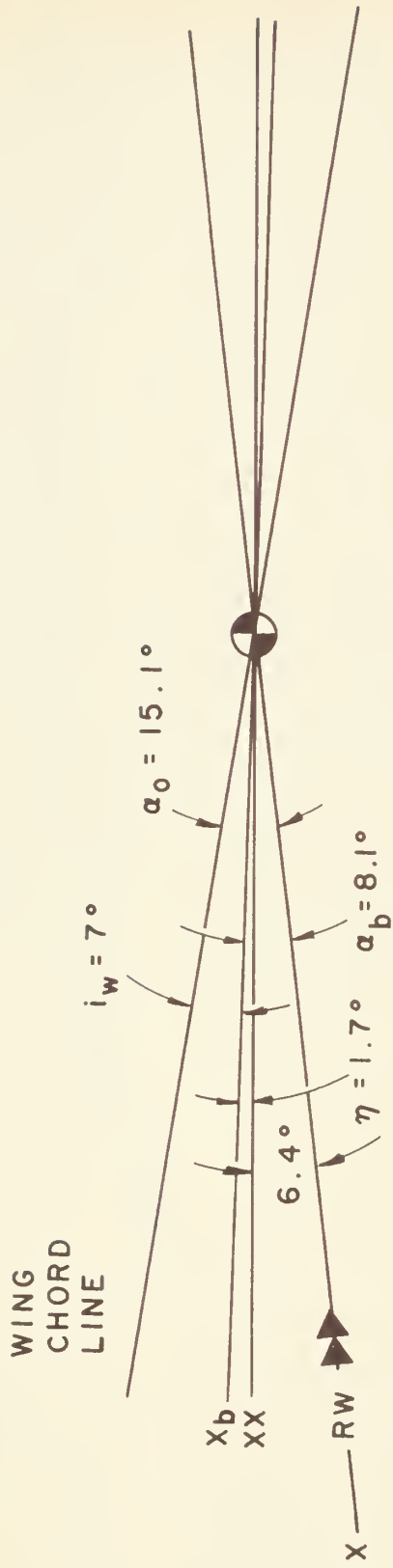
FIGURE 3

LONGITUDINAL ANALOG COMPUTER DIAGRAM









$X_b$  : BODY REFERENCE AXIS  
 $XX$  : PRINCIPAL AXIS  
 $X$  : STABILITY AXIS

FIGURE 5  
 F-8 AIRPLANE X - AXIS



EXACT FUNCTION : APPROXIMATE FUNCTION :

$$\frac{\delta_r}{n_y} = \frac{0.231 S (\frac{S}{5.45} + 1)}{(\frac{S}{1.735} + 1)(\frac{S}{13.6} + 1)}$$

$$\frac{\delta_r}{n_y} = \frac{.231 S}{(\frac{S}{3.2} + 1)}$$

20 LOG  $\frac{AR}{.23} \sim \text{db}$

$A(j\omega)$  EXACT  
 $A(j\omega)$  APPROX.

PHASE  $(j\omega)$  APPROX.

PHASE  $(j\omega)$  EXACT

PHASE

10<sup>3</sup> 0°

$\omega \sim$  RADIANS / SECOND

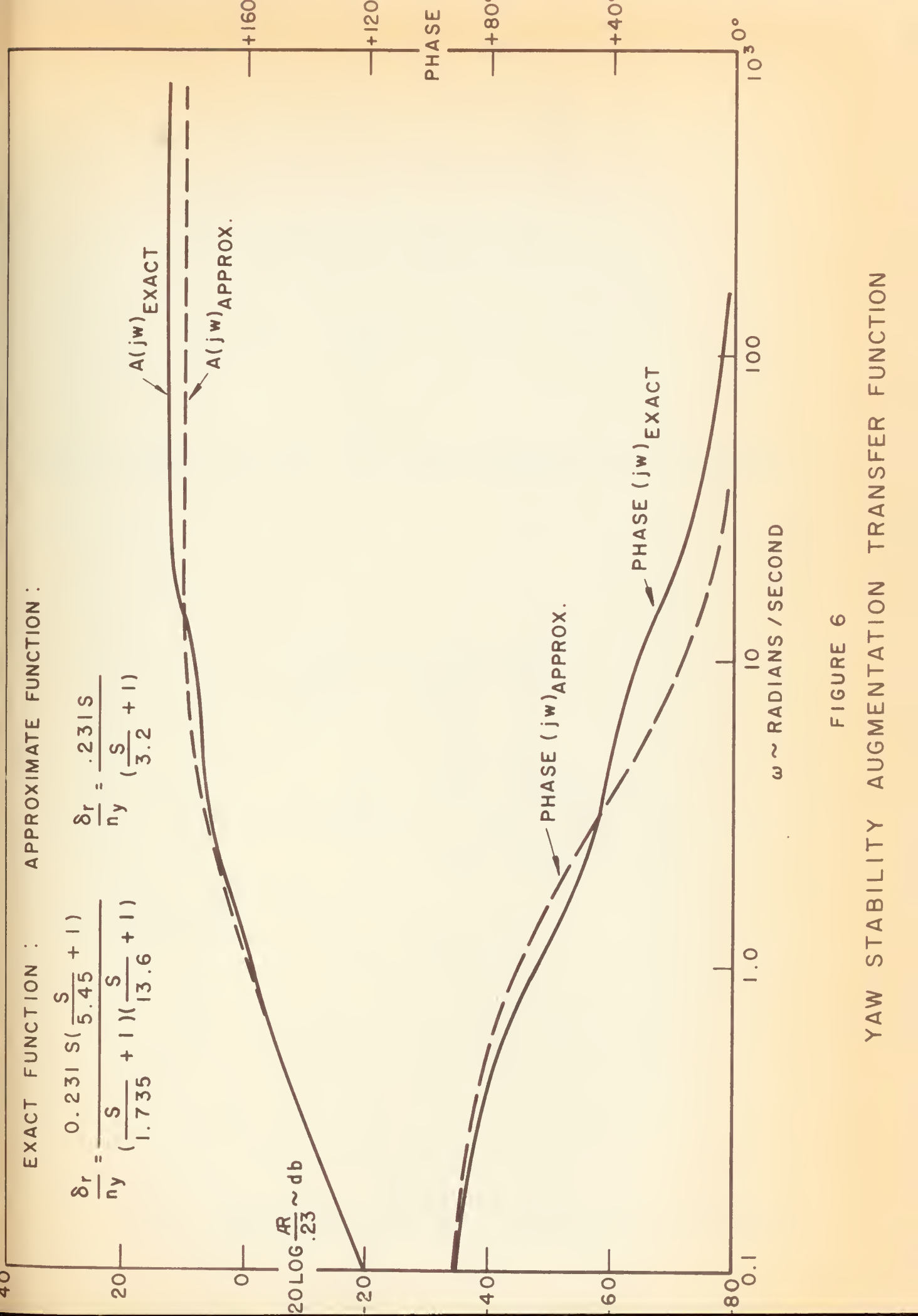


FIGURE 6

YAW STABILITY AUGMENTATION TRANSFER FUNCTION



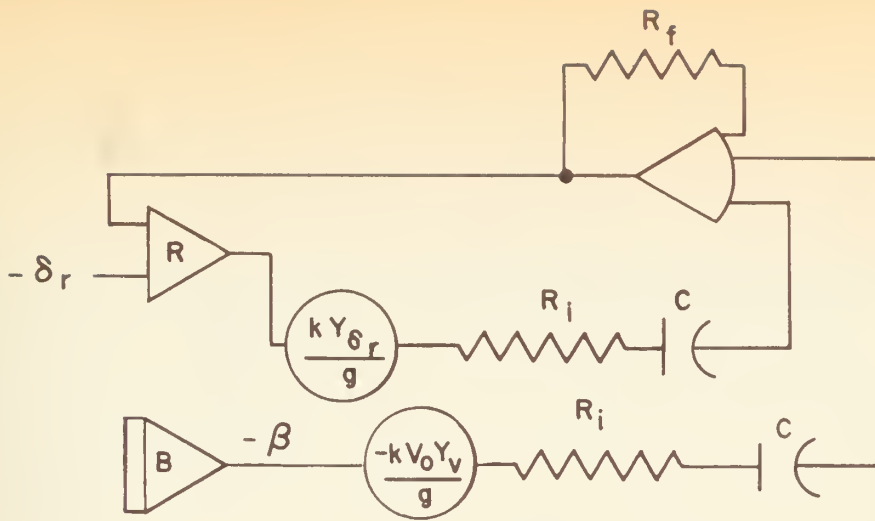


FIGURE 7

YAW STABILIZATION SYSTEM COMPUTER DIAGRAM

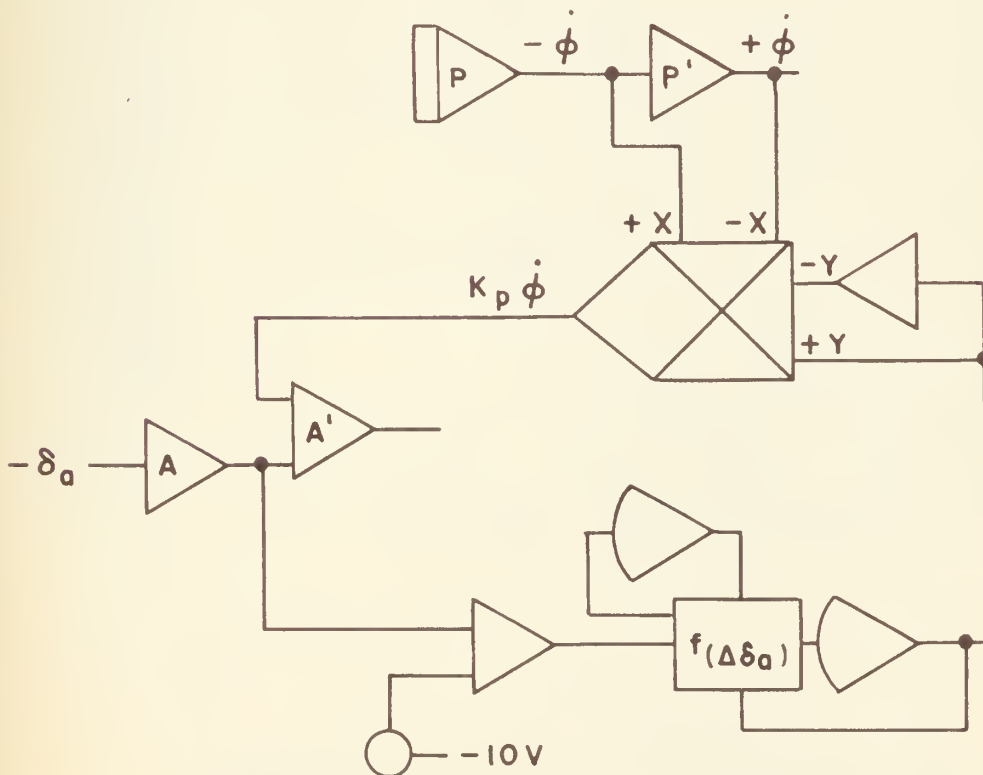


FIGURE 9

ROLL DAMPER SYSTEM COMPUTER DIAGRAM



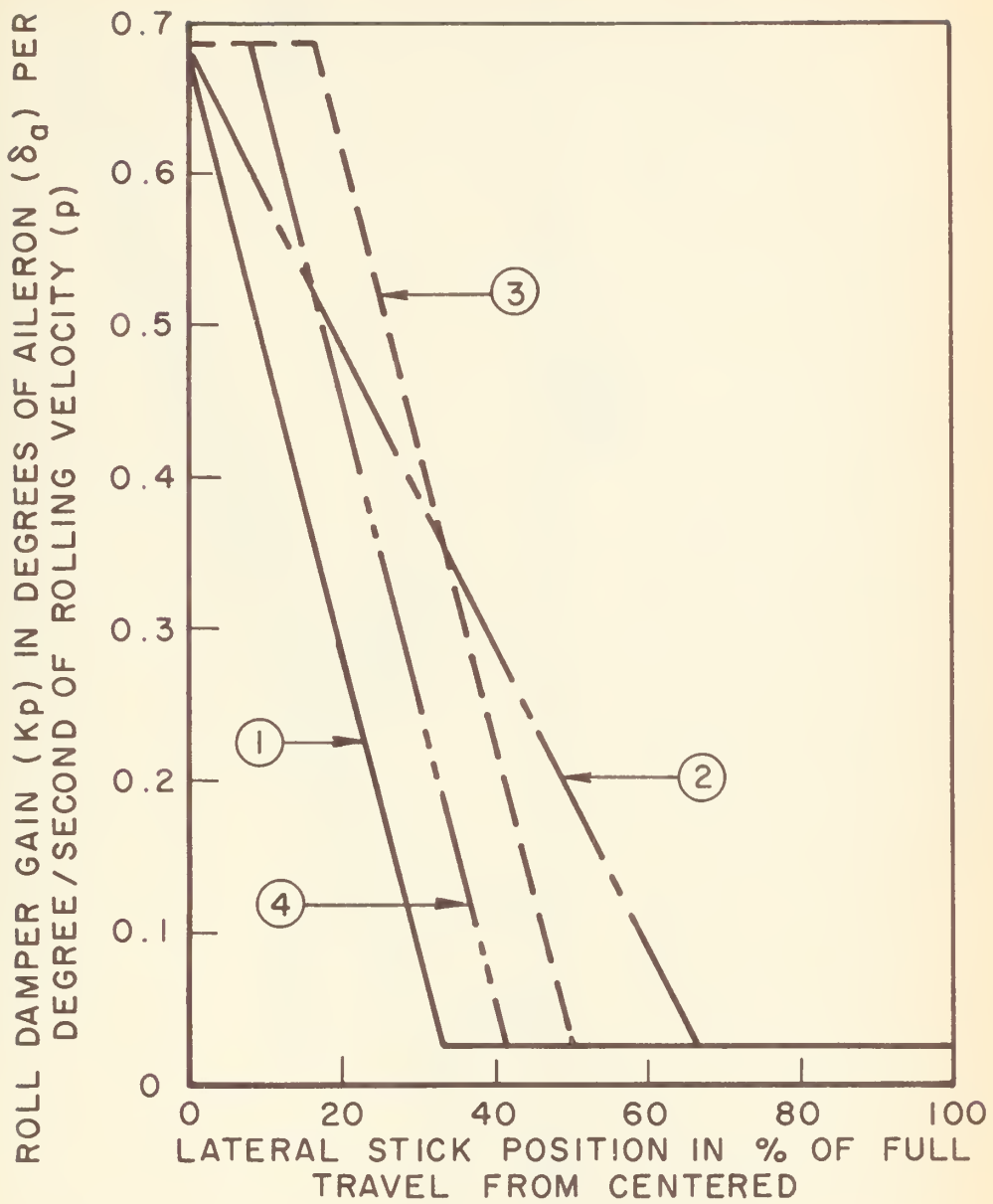


FIGURE 8  
 VARIATION OF ROLL DAMPER GAINS WITH  
 LATERAL STICK POSITION



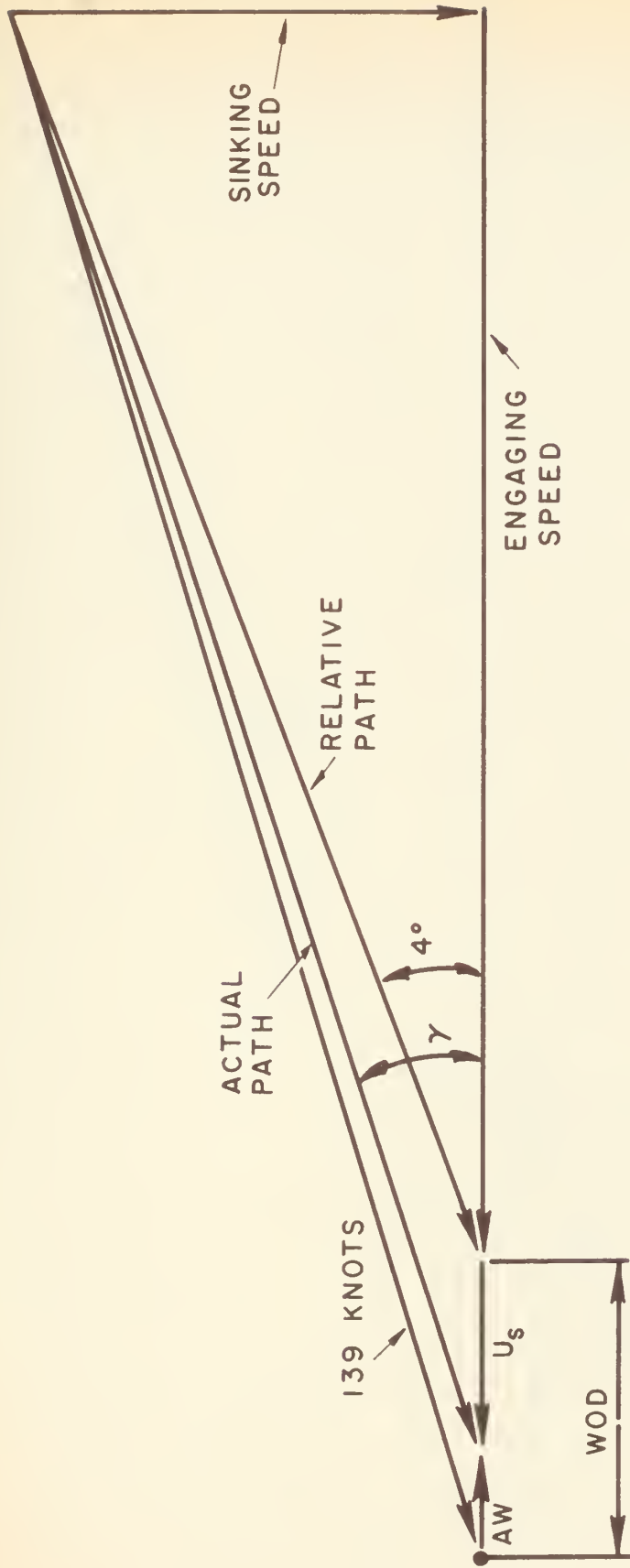


FIGURE 10

VECTOR DIAGRAM OF APPROACH



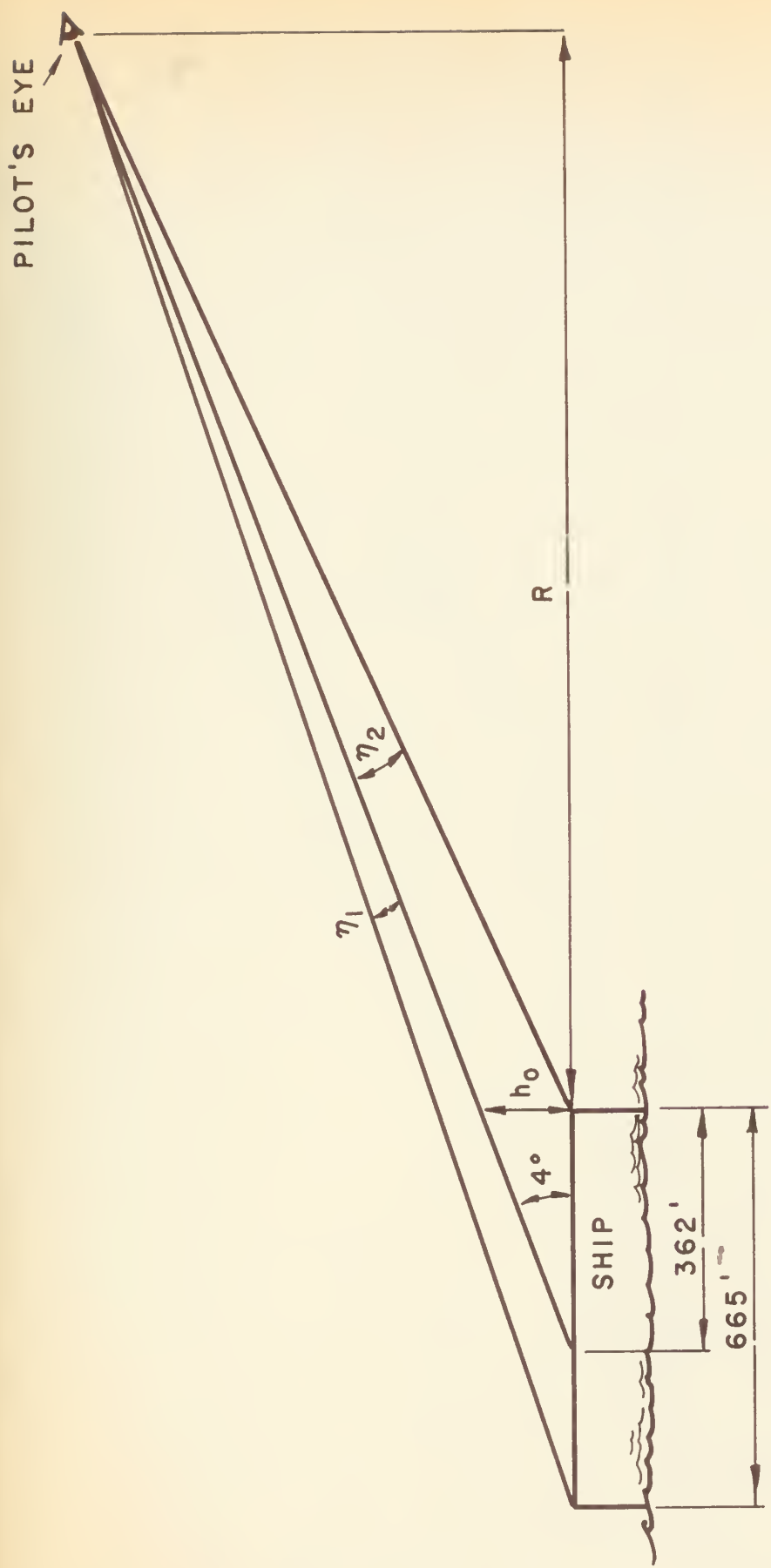


FIGURE 11  
 DETAILS OF THE RELATIVE FLIGHT PATH



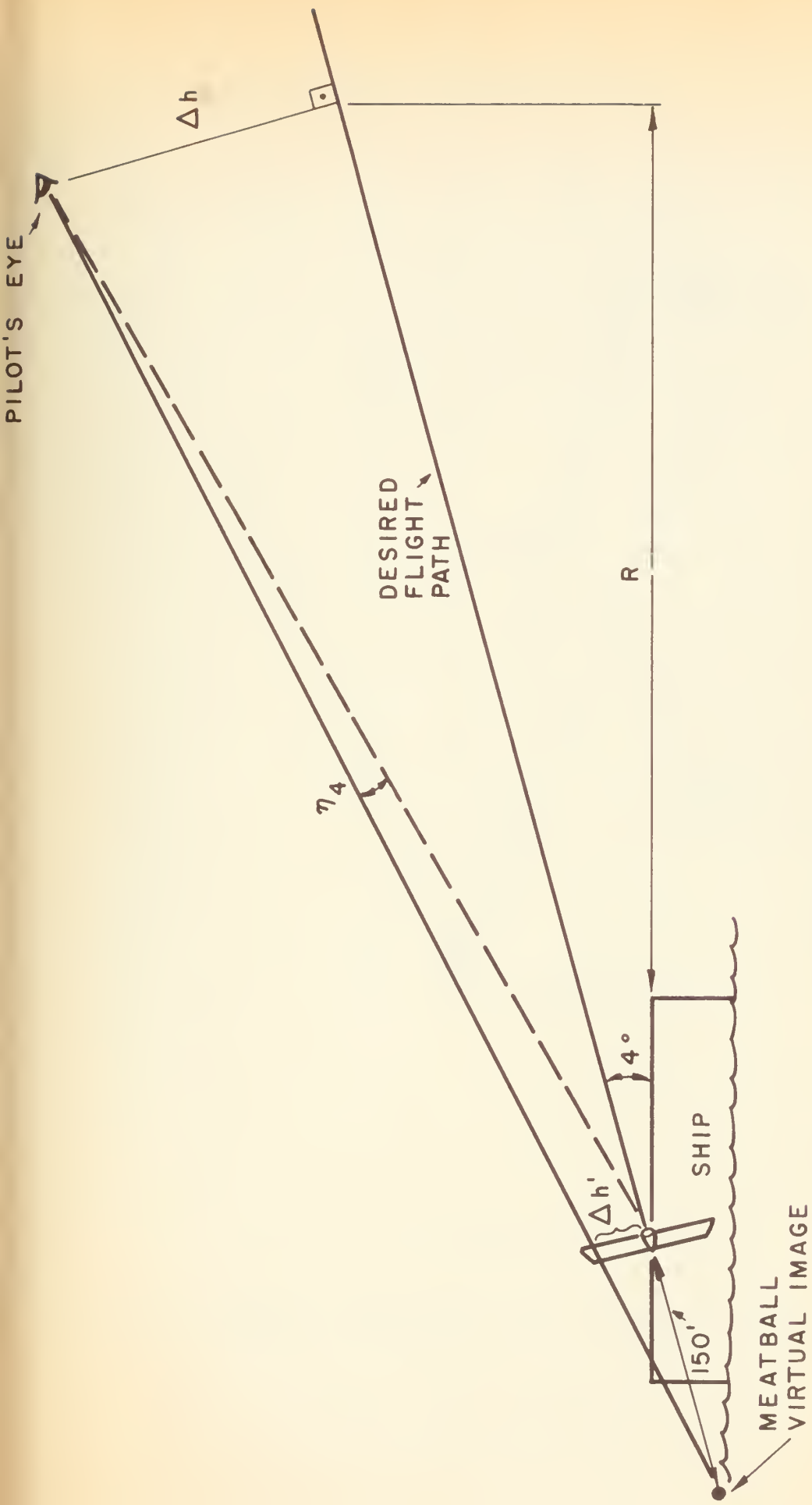


FIGURE 12  
 FRESNEL LENS OPTICAL LANDING SYSTEM GEOMETRY



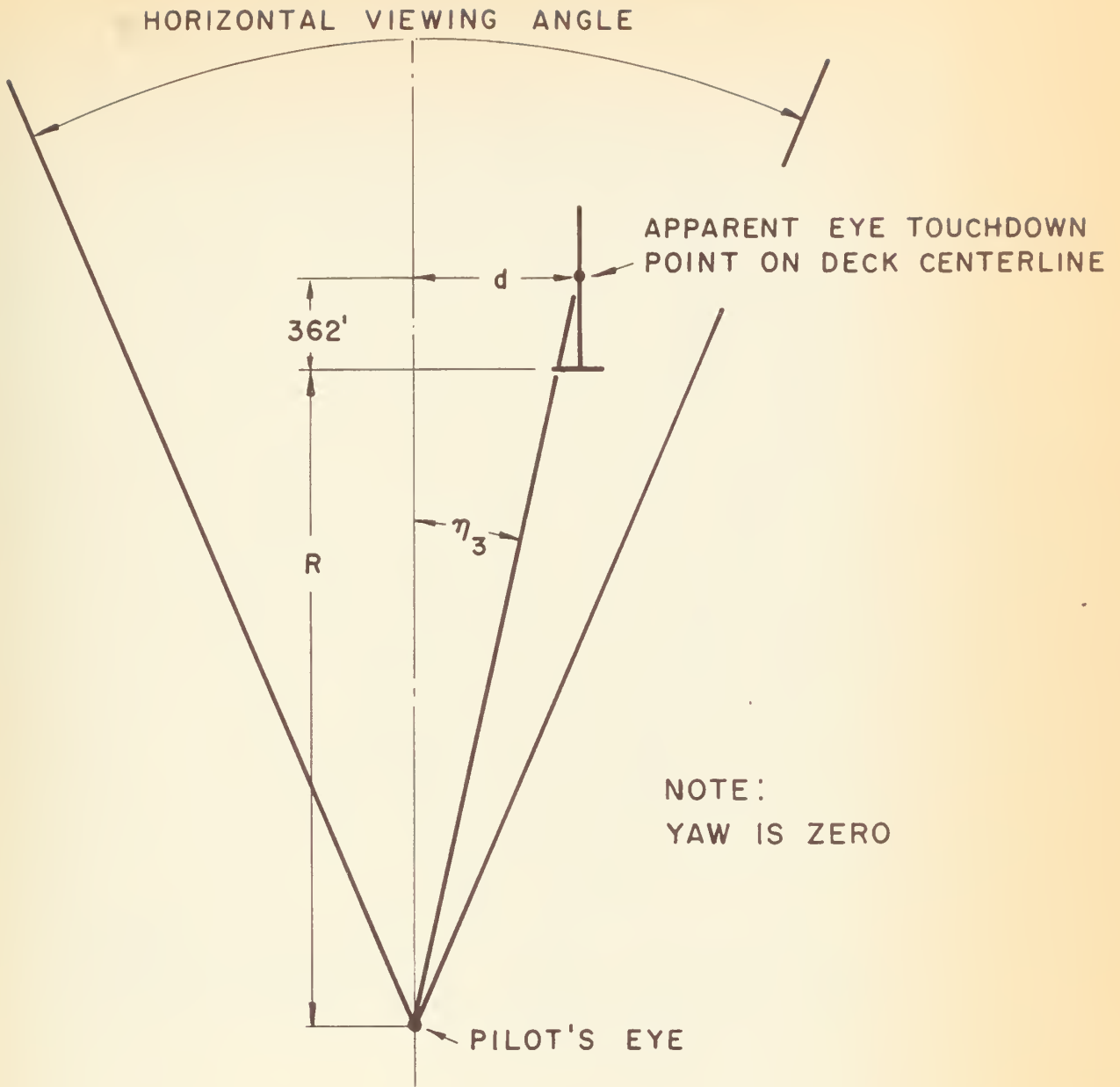


FIGURE 13

PILOT'S VISUALIZATION OF LATERAL DISPLACEMENT



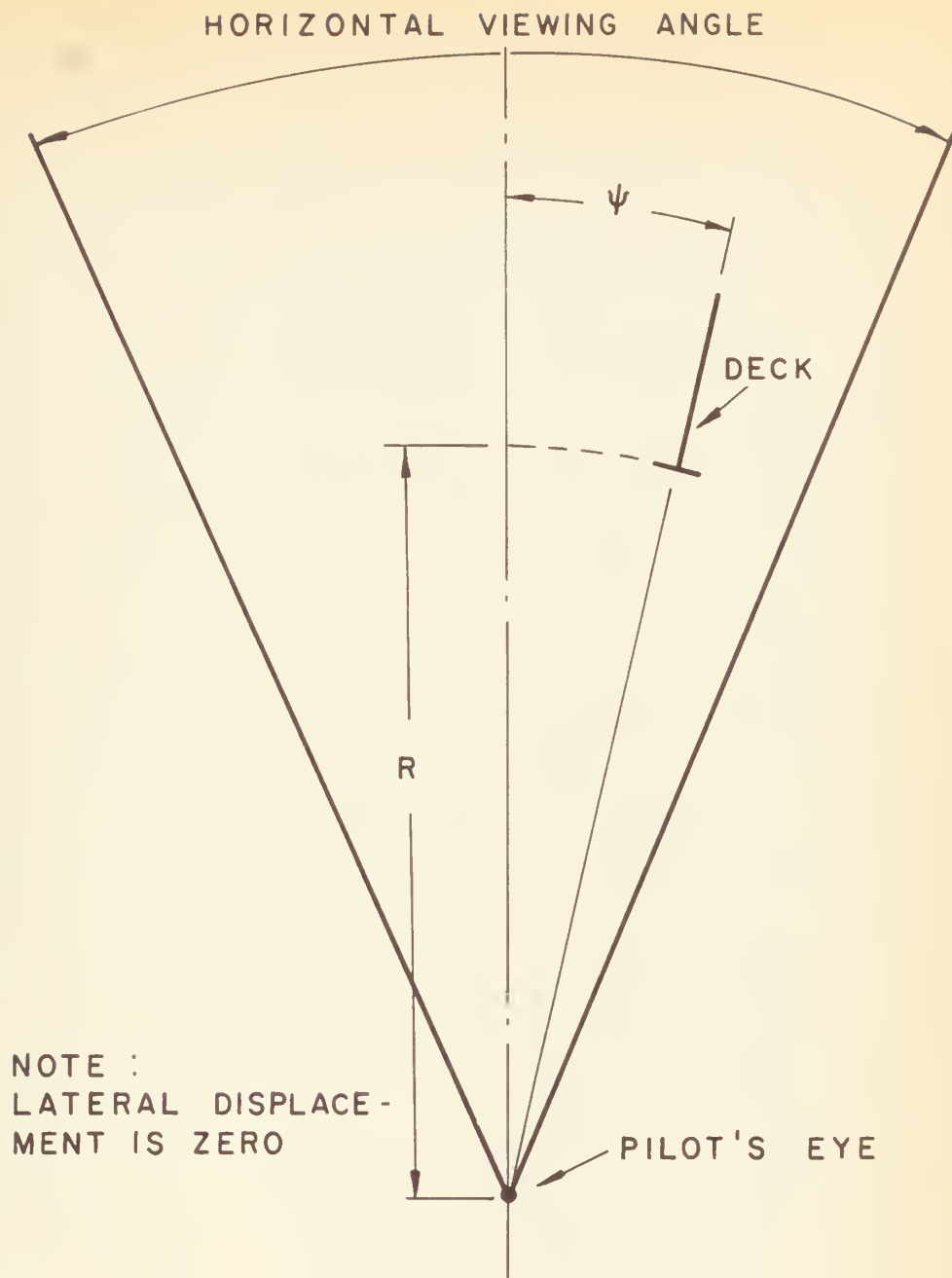
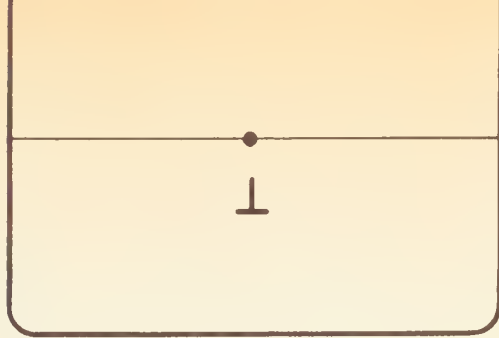


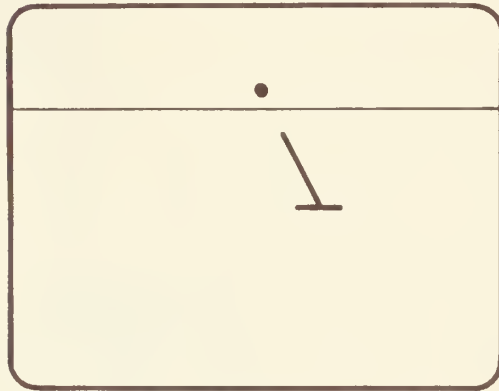
FIGURE 14

PILOT'S VISUALIZATION OF YAW

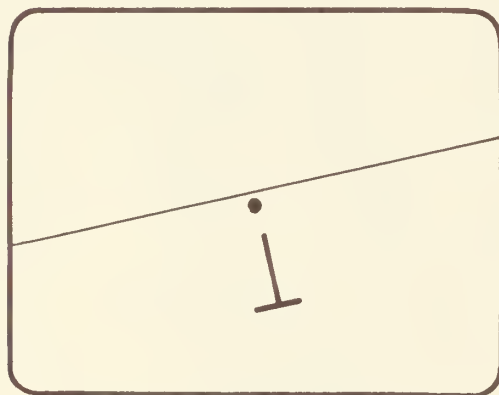




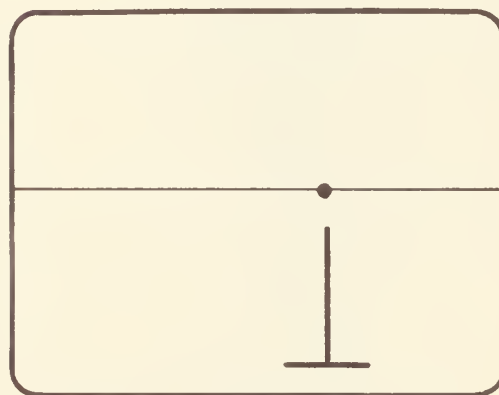
15A



15B



15C



15D

FIGURE 15

CARRIER APPROACH SIMULATOR DISPLAY



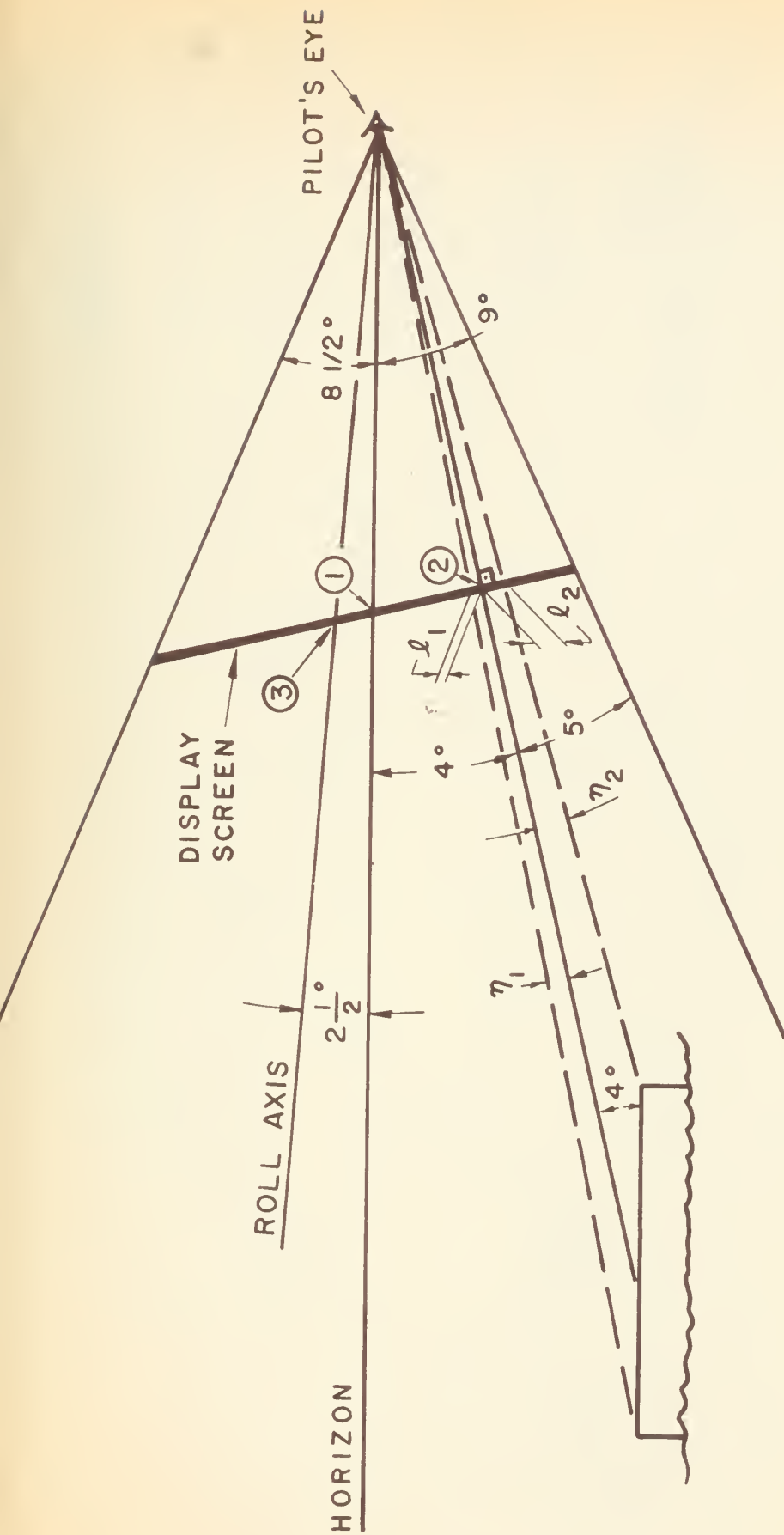


FIGURE 16

VIEWING ANGLE THROUGH FRONT WINDSCREEN DURING CARRIER APPROACH



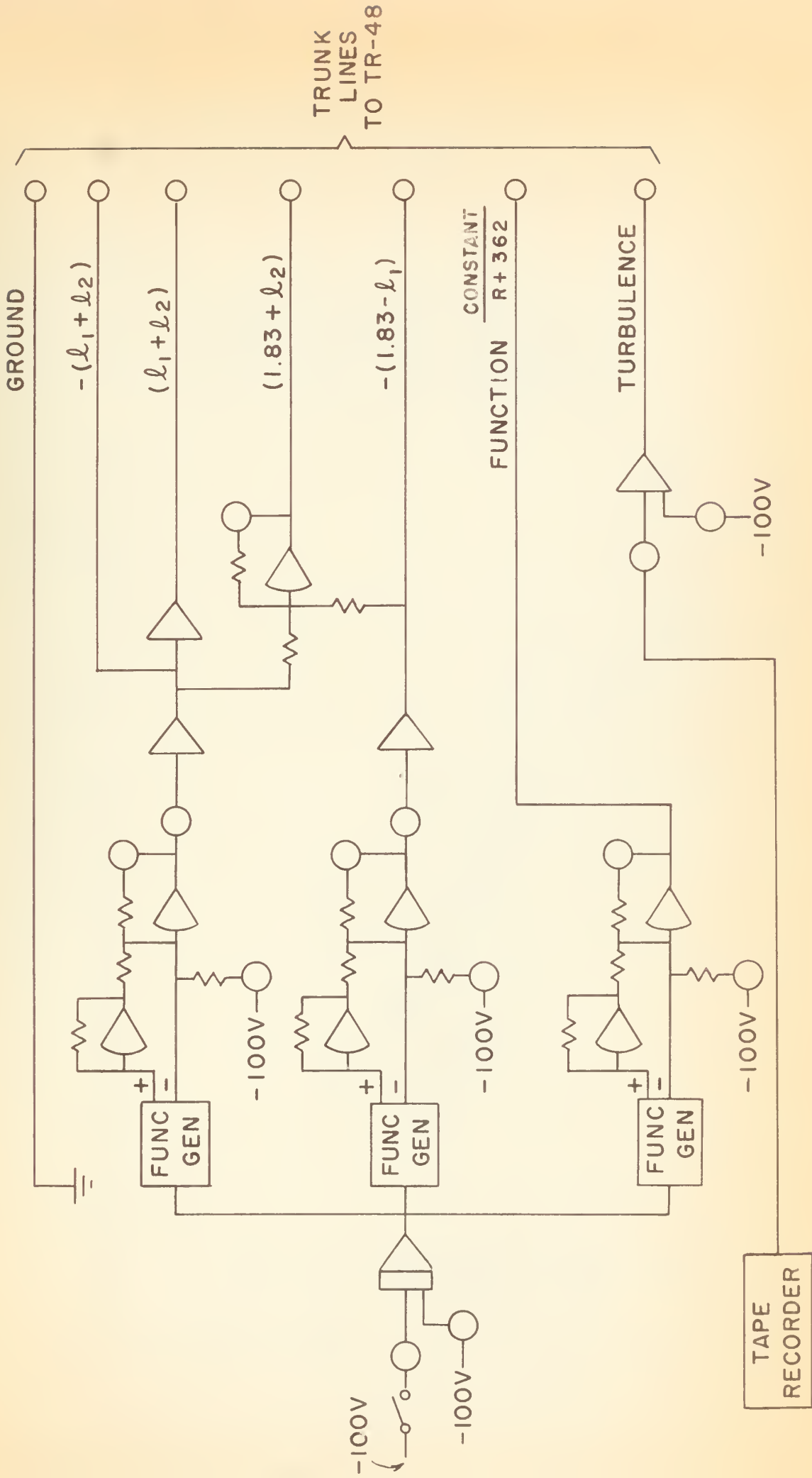
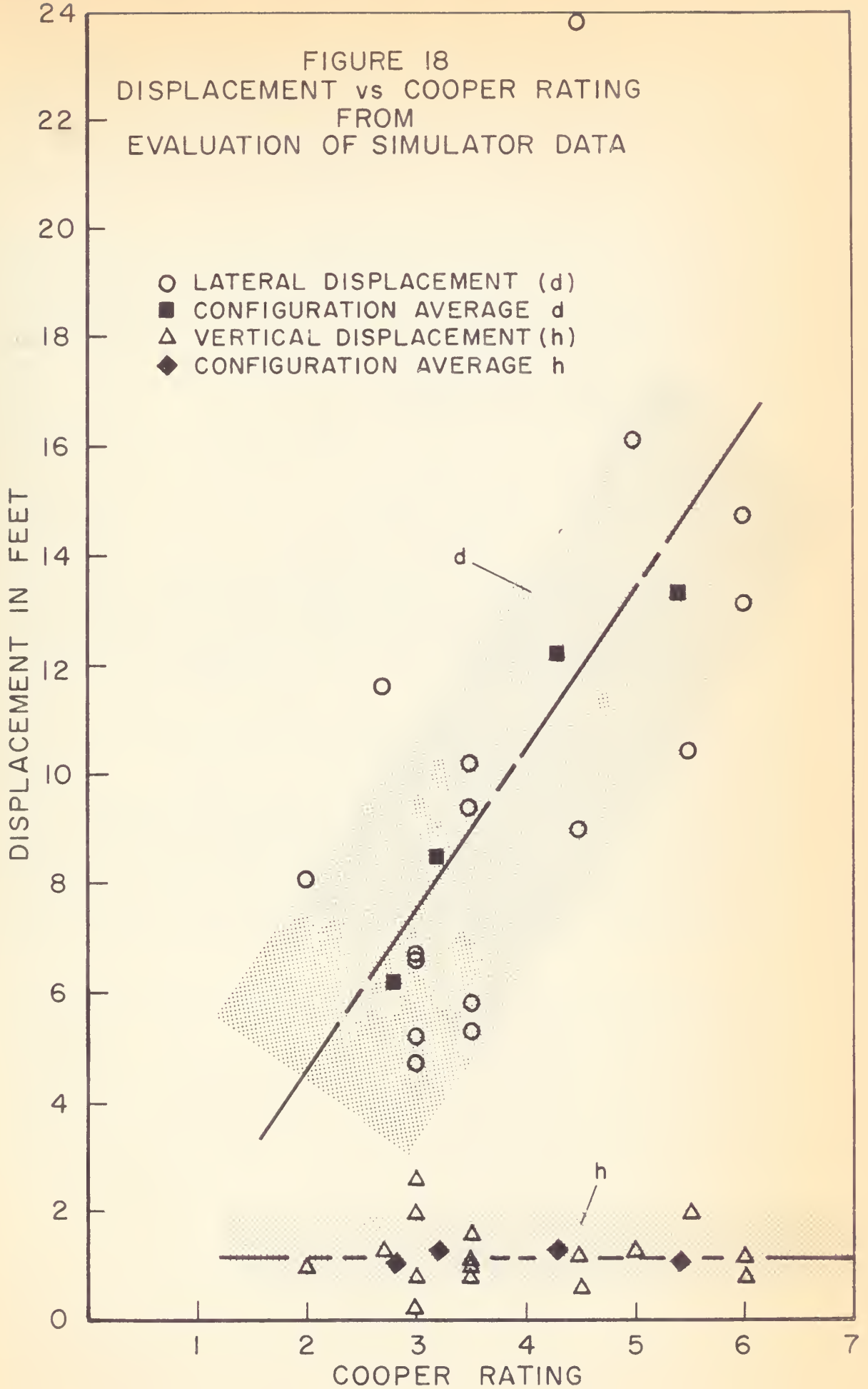


FIGURE 17

DONNER COMPUTER SET-UP



FIGURE 18  
DISPLACEMENT vs COOPER RATING  
FROM  
EVALUATION OF SIMULATOR DATA





$h - .37$  feet/line

$\beta_g$  gust level 1.5 (Table VI)

Figure 19  
TYPICAL TIME HISTORY OF SIMULATED APPROACH  
(moderate turbulence)

time - seconds

5

10

15

20

25

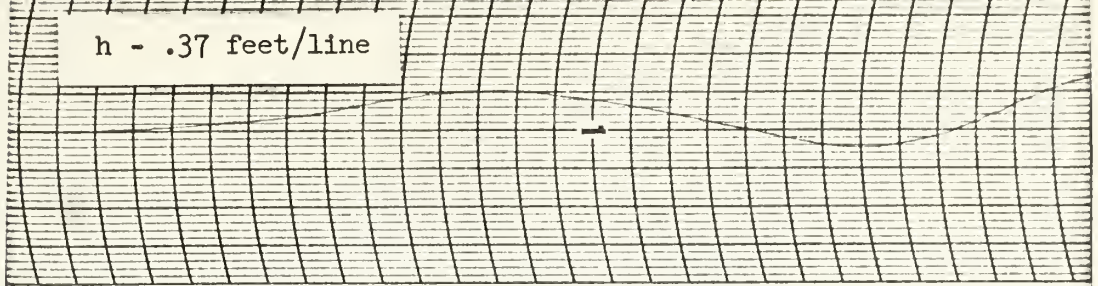
$\varphi$  1.91 degrees/line

$\psi$  .48 degrees/line

$d$  1.27 feet/line



h - .37 feet/line



$\beta_g$  gust level 3.0 (Table VI)

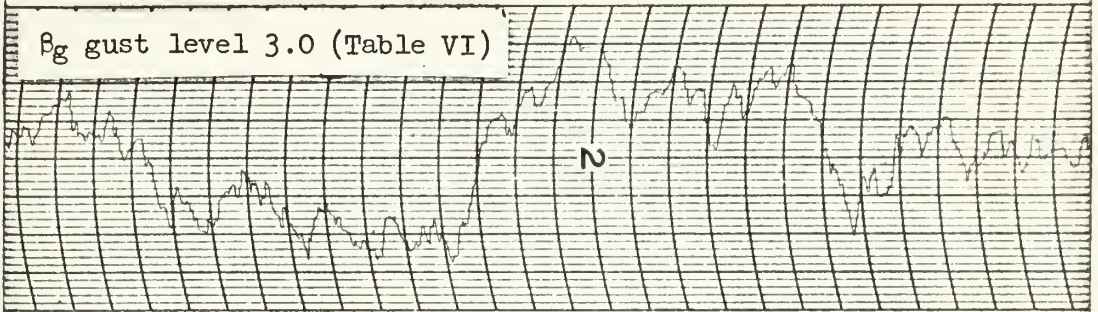


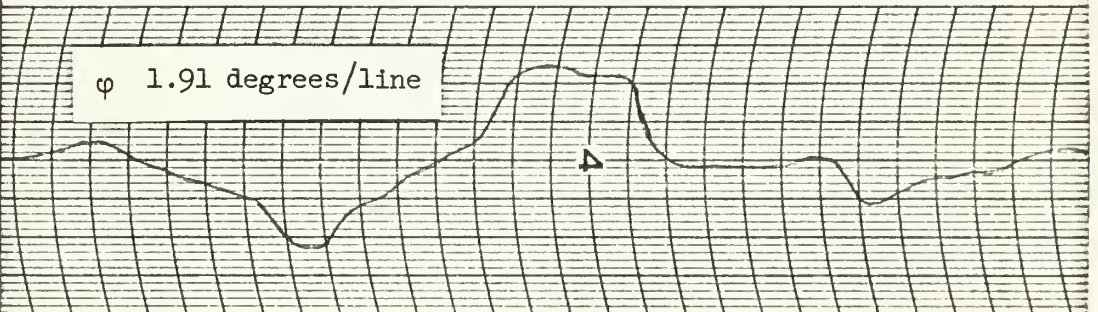
Figure 20  
TYPICAL TIME HISTORY OF SIMULATED APPROACH  
(severe turbulence)

$\omega$

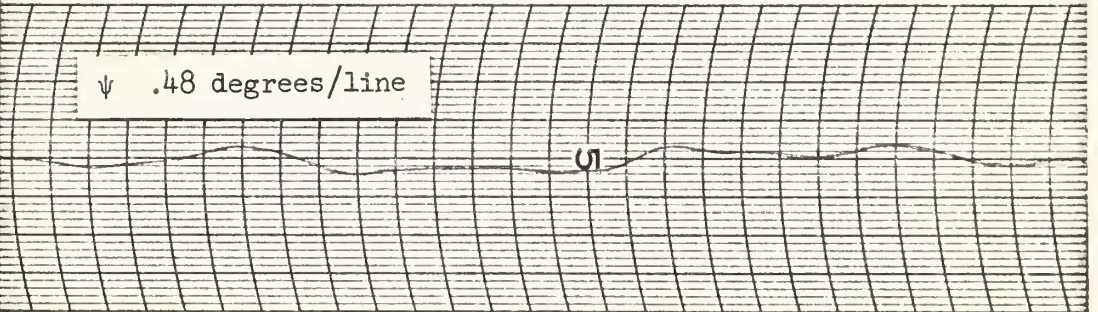
time - seconds

5 10 15 20 25

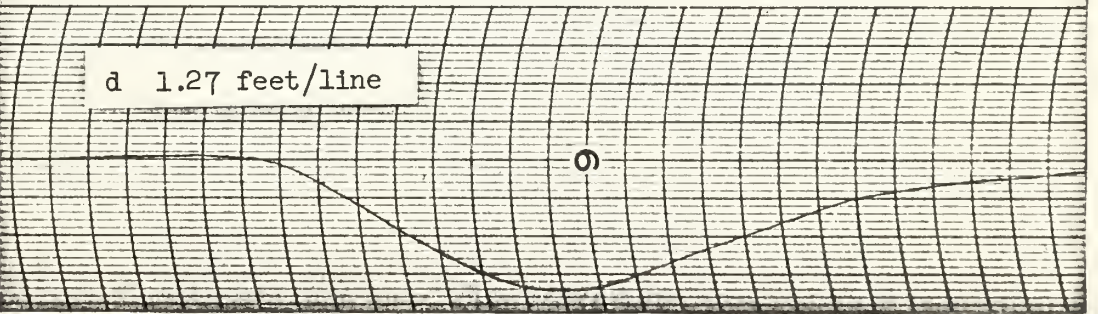
$\phi$  1.91 degrees/line



$\psi$  .48 degrees/line



d 1.27 feet/line







thesF446

A simulator study of a nonlinear roll da



3 2768 002 00169 5

DUDLEY KNOX LIBRARY